High-Resolution Airborne

Geophysical Report on the RP Claims (YC97001-YC97336)

NTS 115O/05 & 115N/08

Claims centered on:

549300E, 7023400N

Latitude: 63°20'N
Longitude: 140°1'W

Registered Owner: Shawn Ryan

Dawson Mining District

Yukon Territory

Dates work performed:

Between June 22nd and August 2nd 2010

Prepared for Kinross Gold Corporation by Lucy Hollis

Submitted 22nd November, 2010

Contents

List of Figures

List of Tables

EXECUTIVE SUMMARY

The RP Claims (1 through 336) are owned by Kinross Gold Corporation (100%) and cover approximately 63.5 km^2. The property is located approximately 75 km south of Dawson City, in the Yukon Territory of Canada. The project area is primarily underlain by deformed and regionally metamorphosed greenschist to amphibolite facies metasedimentary and metaigneous rocks of Palaeozoic and Proterozoic age (Mortensen, 1992; Dusel-Bacon, 2006). During 2010 Kinross Gold Corporation contracted a high sensitivity airborne magnetic and gamma-ray spectrometric survey out to New-Sense Geophysics Ltd. over the RP Claim Block. A total of 1053 km of magnetic lines were flown over the RP Block. The magnetic survey yielded a number of magnetic anomalies and magnetic lineaments. The spectrometric survey, comprising the radioelements K, U and Th produced several high areas on the Claim Block which require further correlation with bedrock geology. Further geological mapping and prospecting, in conjunction with geochemical surveys are warranted to define possible mineralized targets on the RP claims.

1.0 INTRODUCTION

This report describes the logistics of the survey, equipment used; field procedures, data acquisition and results and interpretations for a high sensitivity helicopter magnetic and gamma-ray spectrometric survey carried out on the RP claims, located in the Yukon Territory, Canada. The survey was conducted between June 22nd and August 2nd 2010 by New-Sense Geophysics Ltd. The survey was conducted in a Northwest-Southeast direction. A total of 1053 km of survey line was flown over the RP Claims. Data processing undertaken by New-Sense Geophysics Ltd. involved data compilation, gridding and contouring of geophysical data collected. The proximity of the RP Claims to the recently discovered Golden Saddle Deposit makes the area potentially prospective for mineral exploration.

Unless otherwise stated the coordinate system used is NAD 83, North America (all Canada and USA subunits), Zone 7N.

2.0 SUMMARY OF PREVIOUS INVESTIGATIONS

A small-scale ridge and spur soil survey (called WTwest) was put in across the RP claims by Shawn Ryan, which consisted of the collection of a total of 128 soil samples.

Mapping of the Stewart River area (NTS 115 N, O) was undertaken by the Geological Survey of Canada (GSC) (Ryan and Gordey, 2001; 2004) and published as a geology map in 2004 as part of the Ancient

Pacific Margin NATMAP Project (Figure 3). The regional mapping across the RP claims produced a map dominated by packages of muscovite schist, amphibolite gneiss and variations of felsic gneiss (augen gneiss and grey gneiss). A large, approximately north-south trending Eocene age porphyry body is mapped at the eastern margin of the claim block (Figure 3), with smaller, similar composition igneous bodies located to the northwest. The amphibolite gneiss in the southeastern part of the claim block is punctuated by rhyodacite (Carmacks Group), conglomerate and ultramafic-gabbro.

3.0 PROPERTY INFORMATION

The RP Claims are located in the Dawson Mining District of the Yukon Territory, Canada (Figure 1). The Claims are located approximately 75 km south of Dawson City, Yukon, Canada.

The property consists of 336 full size quartz claims staked on June 23rd, 24th and 25th 2009 by Ryanwood exploration on behalf of Underworld Resources, according to the Yukon Quartz Mining Act (Figure 2). The claims are registered with the Dawson Mining Recorder and are now owned 100% by Kinross Gold Corporation. The RP Claims are shown on Yukon Quartz NTS mapsheets 115O/05 and 115N/08. A full list of claim data is outlined in Table 1. Several of the claims are in conflict; two companies staked the same ground. This issue is still awaiting resolution with the Mining Recorder office in Dawson City.

3.1 Adjacent Claims

The RP Claims surround a block of full size quartz claims: EMC 1 to EMC 32 (grant numbers YD05967 to YD05998) (Figure 2). These adjacent claims are 100 % owned by Archer Cathro & Associates (1981) Ltd. and were staked on June 20th 2009.

3.2 Physiography

The property is located in the White Gold District of the Yukon Territory, Canada. It is characterized by plains incised by streams into V-shaped valleys with interconnecting ridges. Elevation ranges from 1900 feet at valley bottom (18 mile creek) to 4100 feet at ridge tops. Treeline is at approximately 1200 metres. The RP claims are located approximately 24 km northwest of the junction of the White River and the Yukon River, and 35 km in the same direction from the Golden Saddle deposit.

The headwaters of 10 mile creek are located at the western margin of the RP Claims (Figure 2). Similarly 18 mile creek is located at the southwest portion of the RP Claim Block (Figure 2). The area escaped the last two episodes of glaciation.

3.3 Climate

The climate in the Yukon is characterized by low precipitation and a wide temperature range. Winters are cold, and temperatures of -30°C to -40°C are common. Summers are moderately cool to hot, with daily high temperatures of 10°C to 25°C. The property is typically free of snow from late May to the end of September, and the creeks keep flowing from May until October.

Figure 1: Location map showing the study area: RP Claims (in Red), located approximately 75 km south of Dawson City, Yukon

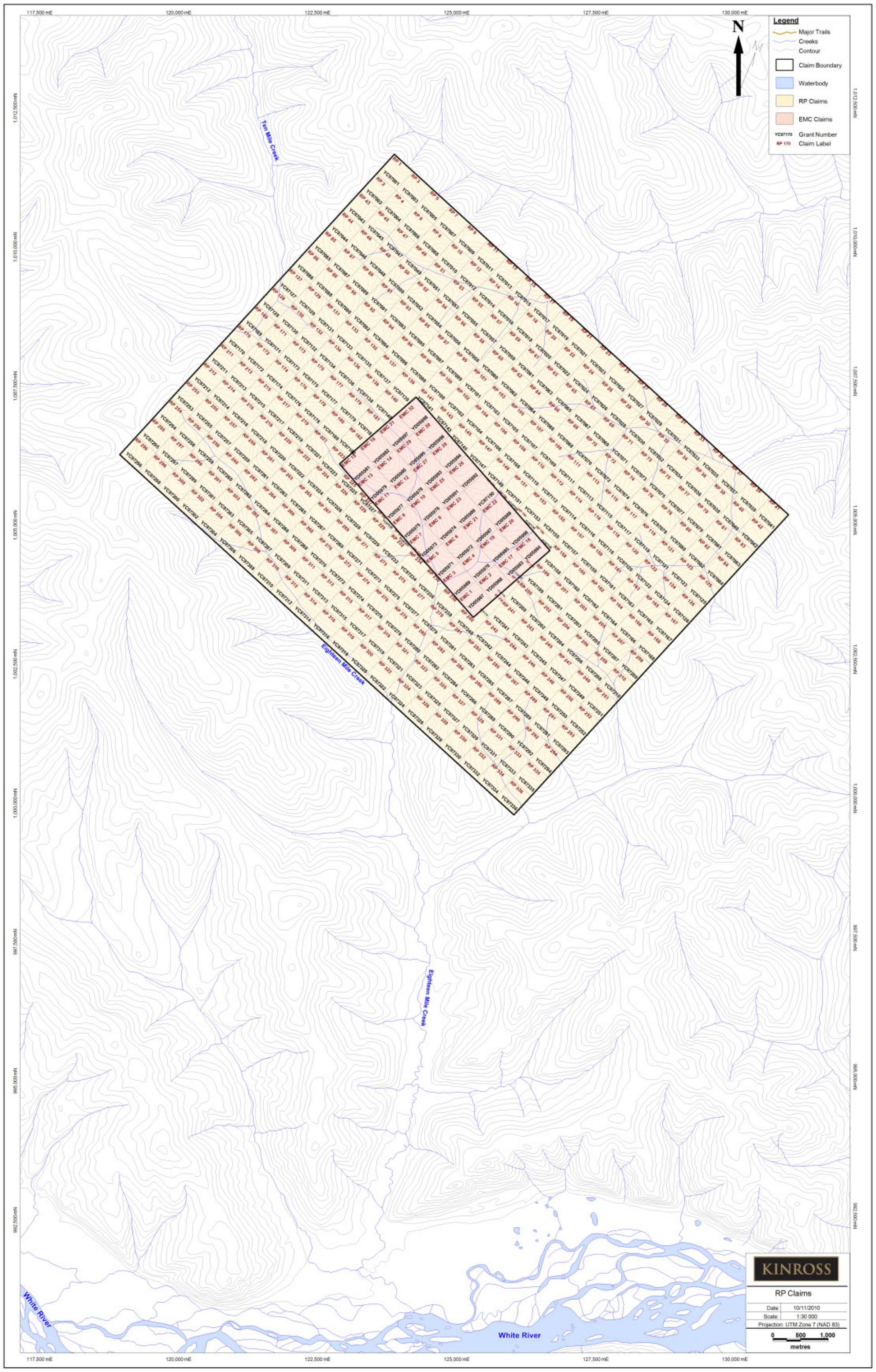

Figure 2: Map showing the RP 1-336 Claims (orange) and adjacent EMC 1- 32 claims (pink)

Claim	Grant # (From)	Grant # (To)	Claim # (From)	Claim # (To)	Reg Type	District	Claim Owner	Operation Recording Date	Staking Date	Claim Expiry Date	Status	NTS Map #	Ops # (From)	Ops # (To)
RP	YC97001	YC97138	1	138	Quartz	Dawson	Shawn Ryan - 100%	6/30/2009	6/23/2009	6/30/2011	Active	115O05	199429	199675
RP	YC97139	YC97139	139	139	Quartz	Dawson	Shawn Ryan - 100%	6/30/2009	6/23/2009	6/30/2011	Application Pending	115O05	199676	199676
RP	YC97140	YC97147	140	147	Quartz	Dawson	Shawn Ryan - 100%	6/30/2009	6/23/2009	6/30/2011	Active	115O05	199677	199684
RP	YC97148	YC97148	148	148	Quartz	Dawson	Shawn Ryan - 100%	6/30/2009	6/23/2009	6/30/2011	Application Pending	115O05	199685	199685
RP	YC97149	YC97149	149	149	Quartz	Dawson	Shawn Ryan - 100%	6/30/2009	6/23/2009	6/30/2011	Active	115O05	199686	199686
RP	YC97150	YC97150	150	150	Quartz	Dawson	Shawn Ryan - 100%	6/30/2009	6/23/2009	6/30/2011	Application Pending	115O05	199687	199687
RP	YC97151	YC97151	151	151	Quartz	Dawson	Shawn Ryan - 100%	6/30/2009	6/23/2009	6/30/2011	Active	115O05	199688	199688
RP	YC97152	YC97152	152	152	Quartz	Dawson	Shawn Ryan - 100%	6/30/2009	6/23/2009	6/30/2011	Application Pending	115O05	199689	199689
RP	YC97153	YC97153	153	153	Quartz	Dawson	Shawn Ryan - 100%	6/30/2009	6/23/2009	6/30/2011	Active	115O05	199690	199690
RP	YC97154	YC97154	154	154	Quartz	Dawson	Shawn Ryan - 100%	6/30/2009	6/23/2009	6/30/2011	Application Pending	115O05	199691	199691
RP	YC97155	YC97155	155	155	Quartz	Dawson	Shawn Ryan - 100%	6/30/2009	6/25/2009	6/30/2011	Active	115O05	199692	199692
RP	YC97156	YC97156	156	156	Quartz	Dawson	Shawn Ryan - 100%	6/30/2009	6/25/2009	6/30/2011	Application Pending	115O05	199693	199693
RP	YC97157	YC97180	157	180	Quartz	Dawson	Shawn Ryan - 100%	6/30/2009	6/25/2009	6/30/2011	Active	115O05	199694	199717
RP	YC97181	YC97197	181	197	Quartz	Dawson	Shawn Ryan - 100%	6/30/2009	6/24/2009	6/30/2011	Application Pending	115O05	199718	199874
RP	YC97198	YC97222	198	222	Quartz	Dawson	Shawn Ryan - 100%	6/30/2009	6/25/2009	6/30/2011	Active	115O05	199875	199899
RP	YC97223	YC97240	223	240	Quartz	Dawson	Shawn Ryan - 100%	6/30/2009	6/24/2009	6/30/2011	Application Pending	115O05	199900	199917
RP	YC97241	YC97336	241	336	Quartz	Dawson	Shawn Ryan - 100%	6/30/2009	6/25/2009	6/30/2011	Active	115O05	199918	200013

Table 1: List of the RP Claims: Displaying grant numbers, Claims numbers, Owner, Expiration date and status (Active in grey)(taken from Yukon mining recorder; claims database)

3.4 Accessibility

The survey area is located approximately 75 km south of Dawson City. Access to the claim at the present time is by helicopter from Dawson City. The Thistle Creek airstrip is the nearest landing zone (43 km to the southeast) for aircraft and crew and gear can be mobilized from this point.

4.0 REGIONAL GEOLOGY

The RP claims are located within the Yukon-Tanana Terrain (YTT), which spans part of the Yukon Territory and east-central Alaska. This terrane is part of the Intermontane Superterrane, and is bounded to the northeast by the right-lateral Tintina-Kaltag and to the southwest by the Denali-Farewell fault systems. The Yukon-Tanana Terrane is composed of deformed and regionally metamorphosed greenschist to amphibolite facies metasedimentary and metaigneous rocks of Palaeozoic and Proterozoic age (Mortensen, 1992; Dusel-Bacon, 2006).

4.1 Property Geology

The basement rocks in the White Gold District consist of Palaeozoic schist and gneisses that underwent Palaeozoic deformation, metamorphism, and pervasive recrystallization (Mackenzie *et al.,* 2010). The RP claims are underlain by metasedimentary and metavolcanic rocks that have been affected by lower amphibolite-grade regional metamorphism and ductile deformation. Regional-scale mapping undertaken by Ryan and Gordey (2004) shows large areas of muscovite schist, amphibolite gneiss with areas of undivided grey gneiss dominating the southeastern part of the RP claim block (Figure 3). A north-south trending Eocene porphyry is mapped crossing the claim block to the eastern margin, with smaller intrusive bodies punctuating the bedrock to the west (Figure 3). Ultramafic bodies are mapped in the RP claim block (Figure 3). Pyroxenite bodies intrude the gneissic host rock in the nearby White Gold district and are generally oriented sub-parallel to the metamorphic foliation. Regional metamorphism formed overturned, tight to isoclinal outcrop-scale folds with shallowly-dipping, NNW-trending axial planes). Serpentinite bodies have also been affected by greenschist facies metamorphism, producing a fabric that formed in association with the regional thrust faults (Mackenzie and Craw, 2009). Serpentinite bodies are the locus of extensive post-metamorphic deformation, including tight or isoclinal folding (centimetre to metre-scale).

The RP claims exhibit similar rock packages to those observed at the White Claims, which are located to the southeast (Paulsen et al., 2010). The structural setting of the RP Claims is also comparable to that recorded at the White Claims (Paulsen et al., 2010) and was a likely reason for the initial staking of the RP claim block.

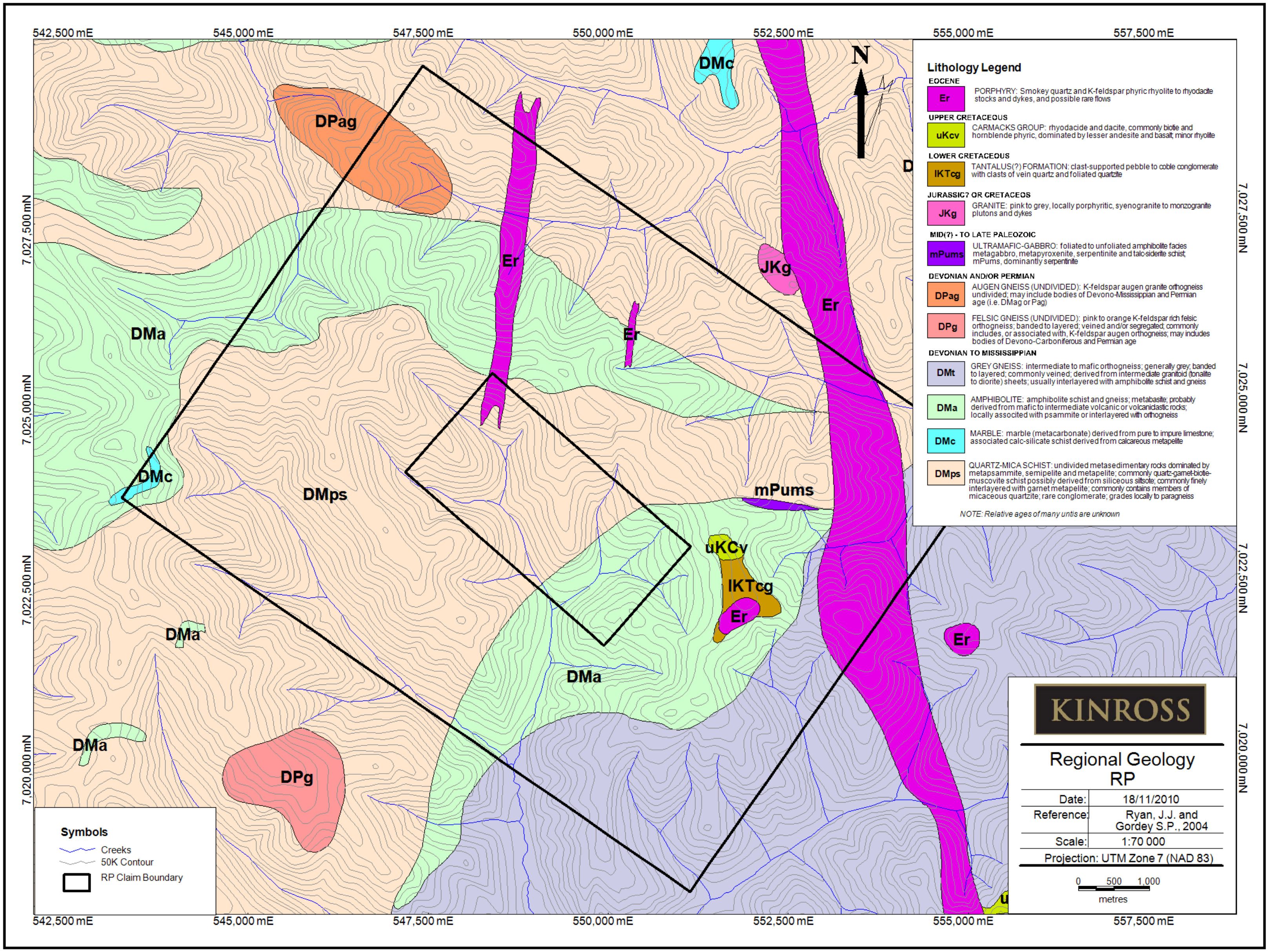

Figure 3: Regional Geology Map for the RP Block and surrounding area (modified from Ryan and Gordey, 2004).

5.0 DESCRIPTION OF GEOPHYSICAL DATA COLLECTED

A high sensitivity helicopter magnetic and gamma-ray spectrometric survey was carried out for Kinross Gold Corp. over a project area and series of claims known as the RP claims and located ~75 km south of Dawson City, Yukon, Canada.

The survey was flown by New-Sense Geophysics (NSG) under the terms of an agreement with the client dated June 1st, 2010. The survey was flown between June 22nd and August 2nd 2010. A total of 1053 km of magnetic and radiometric survey lines were flown over the RP claim block.

RP Block Coordinates are presented below in Table 2:

UTM Nad 83 Zone 7N			
NAD 83_X	**NAD 83_Y**	**WGS84_X**	**WGS84_Y**
543262	7023690	543262	7023690
547501	7029718	547501	7029718
555384	7024088	555384	7024088
551078	7018259	551078	7018259
543262	7023690	543262	7023690

Table 2: Block coordinates for the RP Claim Block.

Survey Parameters:

Traverse Line spacing:	75 m
Control Line spacing:	750 m
Nominal Terrain clearance:	30 m
Average Terrain clearance:	35.7 m (RP block)
Navigation:	Global Positioning System
Traverse Line Direction:	56, 236 deg.
Control Line Direction:	146, 326 deg.
Measurement Interval:	0.1 sec for magnetic
	1.0 sec for radiometrics and GPS
Ground speed (average):	72 km/h (RP block)
Measurement spacing (average):	2.0 metres/0.1 sec, 20.0 metres/1 sec (RP block)
Airborne Digital Record:	Line Number

	Flight Number
	Radar Altimeter
	Total Field Magnetics
	Live Time
	Thorium counts
	Potassium counts
	Uranium counts
	Upward looking Uranium counts
	Cosmic counts
	Down Spectrum
	Total Counts
	Time (System and GPS)
	Raw Global Positioning System (GPS)
	Magnetic compensation parameters (fluxgate mag.)
Base Station Record:	Ambient Total Field Magnetics
	Raw Global Positioning System (GPS) data
	Time (System and GPS)

6.0 PERSONNEL

6.1 Field Operations

New-Sense Geophysics Ltd., Geophysicist:	Sean Plener
New-Sense Geophysics Ltd., Geophysicist:	Chris Evans
Fireweed Helicopter, Pilot:	Brent Vansickle
Fireweed Helicopters, Pilot:	RJ Price

6.2 Office data processing and Offsite QA/QC

QA/QC, Maps, Logistics Report (NSG):	Andrei Yakovenko
QA/QC (Bob Ellis EGG Inc.):	Bob Ellis
Data Processing and Grids:	Andrei Yakovenko, Sean Plener, Chris Evans

6.3 Project Management

New-Sense Geophysics Ltd.:	Andrea Yakovenko
Bob Ellis EGG Inc. (client representative):	Bob Ellis
Kinross Gold Corp.:	Jean-Pierre Londero

7.0 METHOD OF COLLECTION

7.1 Aircraft and Equipment

The aircraft used was a Bell 206B 3 helicopter (C-FFWH) equipped with a Cesium magnetometer mounted in a fixed stinger assembly and RS-500 airborne spectrometer mounted in the storage compartment. Fireweed Helicopters based in Dawson City, Yukon, Canada provided the aircraft service.

7.2 Airborne Geophysical System

7.2.1 Magnetometer

One Scintrex CS-3 optically pumped Cesium split beam sensor was mounted in a fixed stinger assembly. The magnetometer's Lamor frequency output was processed by a KMAG-4 magnetometer counter, which provides resolution of 0.15 ppm (in a magnetic field of 50,000 nT, resolution equivalent to 0.0075 nT). The raw magnetic data was recorded at 50 Hz, anti-aliased with 51 point COSINE filter and re-sampled at 10 Hz.

7.2.2 Magnetic Compensation

The proximity of the aircraft to the magnetic sensor creates a measurable anomalous response as a result of the aircrafts movement. The orientation of the aircraft with respect to the sensor and the motion of the earth's magnetic field are contributing factors to the strength of this response. A special calibration flight, Figure of Merit (i.e. FOM) was flown to record the information necessary to compensate for those effects.

A three-axis Bartington fluxgate magnetometer (recorded at 50 Hz) was used to measure the orientation and rates of change of the magnetic field of the aircraft, away from localized terrestrial magnetic anomalies. The QC Tools digital compensation algorithm was then applied to generate a correction factor to compensate for permanent, induced, and eddy current magnetic responses generated by the aircrafts movements.

7.2.3 GPS Navigation

A U-BLOX RCB-LJ sixteen channel GPS receiver, which is an integral component of the iNav V3 computer system, was used to run the flight control system and provide precise positioning of the aircraft.

7. 2.4 Altimeter

A TRA 3500 radar altimeter was mounted inside with stinger. This instrument operates with a linear performance over the range of 0 to 2,500 feet and records the terrain clearance of the sensors. The raw radar altimeter data was recorded at 50 Hz, anti-analized with a 21 point COSINE filter and re-sampled at 10 Hz.

7.2.5 Geophysical Flight Control System

New Senses's iNAW V3 geophysical flight control system monitored and recorded magnetometer, spectrometer, altimeter, and GPS equipment performance. Input from the various sensors was monitored every 0.005 seconds for the precise coordination of geophysical and positional measurements. The input was recorded fifty times per second.

7.2.6 Spectrometer

The RS-500 Airborne Spectrometer with RSX-5 detector pack, manufactured by Radiation Solutions Inc. (RSI) was used for the survey. The RS-500 spectrometer has a multi-peak gain stabilization algorithm and is capable or recording 1024 channels with accuracy of 0.1 to 10 counts/second.

7.2.7 Idasdigital recording

The output of the CS-3 magnetometer, fluxgate magnetometer, altimeter, temperature, pressure, GPS coordinates, and time (system and GPS), were recorded digitally on a Compact Flash drive at a sample rate of fifty times per second (one time per second for GPS) by the iNAV V3 system.

7.2.8 Pressure and Temperature

A Honeywell Precision Pressure Transducer, model PPT0020AWN2V A-A, was used to record the ambient pressure and temperature during the survey. The device was mounted in the helicopter stinger. The pressure and temperature outputs units were mbar and degrees Celsius respectively.

7.2.9 Spectrometer Digital Recording

The output of the RS-500 spectrometer, GPS coordinates and time (UTC) were recorded digitally on an internal RS-500 flash drive at a sample rate of 1Hz. After each flight the data were copied and synchronized using UTC clock with the iDAS digital records.

7.3 Ground Monitoring System

7.3.1 Base Station Magnetometer

A Scintrex CS-3 optically pumped cesium split beam sensor was used at the base of operations within the airport boundaries, in an area of low magnetic gradient and low/free from cultural electric and magnetic noise sources. The sensitivity and absolute accuracy of the ground magnetometer is ± 0.01 nT. Data was recorded continuously at least every one second throughout all survey operations in digital form on a TC-10 data acquisition system. Both the ground and airborne magnetic readings were synchronized based on the GPS clock.

7.3.2 Recording

The outputs of the magnetic and GPS monitors were recorded digitally on a dedicated TC-10 computer. A visual record of the last three hours was graphically maintained on the computer screen to provide an up-to-date appraisal of magnetic activity. At the conclusion of each production flight raw GPS and magnetic data were transferred to the main field compilation computer.

7.3.3 Field Compilation System

A field laptop computer was used for field data processing and presentation. The raw data was imported to Geosoft Oasis montaj for QA/QC and processing purposes. After checking for quality control, the database and uncompensated magnetic readings were exported to QC Tools software package for magnetic compensation and base station merging purposes.

8.0 PRE-SURVEY SPECTROMETER CALIBRATIONS

Pre-survey calibrations and testing of the RS-500 (SN 5516) airborne gamma-ray spectrometry system were carried out on June 21st, 2010 (at the installation base in Dawson, YT) and June 24th, 25th, 2010 (in the vicinity of the White Gold project property). For these calibration and tests the survey aircraft and configurations were selected to conform to contract technical specifications. Calibration of the spectrometer involved:

- **Calibration Pad measurements**, which are used to determine the “spectral overlap” coefficients. The calibration test was performed within a 12 month period before the survey by the manufacturer (Radiation Solutions Inc.).
- **Cosmic Flight Test**, which was used to determine the aircraft background values and cosmic coefficients (conducted on June 24th, 2010).
- **Height Attenuation Test**, which determined the altitude attenuation coefficients.

8.1 Energy Windows

The airborne radiometric technique requires measurement of count rates for specific energy regions or windows in the natural gamma-ray spectrum. The standard energy regions (in accordance with the International Atomic Energy Agency (IAEA), and their corresponding channel limits are shown in Table 3:

Designation	Energy Limit (keV)		Channel Limit (inclusive) Unit Values	
	Lower	Upper	Lower	Upper
Total Count (TC)	410	2810	137	937
K	1370	1570	457	523
U	1660	1860	553	620
Th	2410	2810	803	937
U (Upward)	1660	1860	553	620
Cosmic	3200	Infinity		

Table 3: Downward Spectrometer Energy Windows

8.2 Calibration Pad Test

The Compton stripping coefficients as provided by RSI are listed in Table 4:

Stripping Ratios	Spectrometer (SN 5516)	‘normal’ values
Th into U (alpha = a23/a33)	0.271	0.250
Th into K (beta = al3/a33)	0.396	0.400
U into K (gamma = a12/a22)	0.75	0.810
U into Th (a = a32/a22)	0.045	0.060
K into Th (b= a31/a11)	0	0
K into U (g=a21/a11)	0	0.003

Table 4: Compton Stripping Coefficients

8.3 Cosmic Flight Test

In each of the spectral windows, the radiation increases exponentially with height due to radiation of cosmic origin. As well, the aircraft contributes a constant background to the count rate. By completing a series of flights within the same region, over a range of altitudes, these background contributions can be determined (Appendix A).

8.3.1 Setup and measurement procedure

A resolution check was completed at the aircraft base using a Thorium source prior to the cosmic test to insure the sensitivity and accuracy of the spectrometer.

Once the aircraft reached the desired altitude (first at ~8000 feet), survey data were recorded for approximately ten minutes. This was then repeated at 9 000, 10 000, 11 000, and 12 000 feet above sea level (Table 5).

	Cosmic Test Flight Data (average counts)					
Altitude (ft)	**Cosmic**	**UU**	**K**	**U**	**Th**	**TC**
8144	172	3	18	10	11	243
9132	223	4	22	13	15	309
10135	259	4	25	15	17	353
11136	304	5	28	18	21	405
12074	353	6	32	20	24	463

Table 5: Cosmic Test Data

8.3.2 Results from Cosmic Flight Test

At each altitude, the raw data for the five windows of interest (Th, K, U, TC, and U Upward) were evaluated for quality. The mean values were then extracted and plotted against the cosmic background window. The results from the graphs (Appendix A) are summarized in Table 6.

	Cosmic Flight Test Result from	
	Cosmic stripping	**Aircraft Background**
K	0.0767	4.8767
U	0.0564	0.4234
Th	0.0674	0
TC	1.2101	37 313
UU	0.0159	0.2207

Table 6: Calculated Cosmic and Aircraft Background Coefficients

8.4 Altitude Attenuation Test

The height attenuation of the spectrometer systems was calculated by flying a series of passes across a line over flat ground with uniform radioelement ground concentration. The test range was flown by acquiring data on a series of seven passes over a set path, at the following altitudes: 100, 150, 200, 250, 300, 400, 600, 800 and 1000 feet above ground.

8.4.1 Results from Altitude Attenuation Test

The airborne data from the altitude attenuation test was checked for quality. The radiometric windows were then corrected for background (aircraft and cosmic) and stripped of Compton contributions. After averaging the data for each line, the four windows of interest (K, U, Th, and Total Count) were plotted against the altimeter in order to obtain the height attenuation (Appendix A).

The results were obtained using an exponential regression where the slope represents the attenuation coefficient and the 'y' intercept represents the counts at 0 feet (

Table 7).

Element	Altitude attenuation coefficients
K	-0.0079
U	-0.005
Th	-0.0081
TC	-0.0062

Table 7: Calculated Height Attenuation Coefficient

8.5 Radon Hover Test

The determination of calibration constants that enable the stripping of the effects of the atmospheric radon from the downward-looking detectors through the use of an upward looking detector is divided into two parts:

1) Determining the relationship between the upward and downward looking detector count rates for radiation due to atmospheric radon. Two test areas were established over an area of flat ground near the base of operations at the White Camp. Each day the aircraft hovered over the test area for ~5 minutes.
2) Determining the relationship between the upward and downward looking detector count rates for radiation originating from the ground using complete survey dataset.

The Upward detector ground component is related to the downward detector ground components be linear equation:

$$u_g = a_1 \, x \, U_g + a_2 x \, T_g$$

Where:

- u_g, U_g and T_g are contribution in the windows that originate from the ground.
- a_1 and a_2 are empirically determined calibration factors.

The procedure, as per IAEA Report # 323, in determining the a_1 and $a_2$factors was applied to the survey block dataset with the following results (Table 8):

a_1	0.051184
a_2	0.027052

Table 8: RP Block a_1 and a_2 factors

9.0 OPERATIONS AND PROCEDURES

9.1 Flight Planning and Flight Path

The block outline coordinates (Table 2) were used to generate pre-calculated navigation files. The navigation files were used to plan flights at the designated traverse line spacing of 75 m and control lines of 750 m.

9.2 Base Station

Magnetic base stations were established in magnetically quiet areas in the vicinity of the White Gold camp (at latitude 63.165897; Longitude: -139.488468) (Figure 4).

Figure 4: Base Station setup located at the White Gold Camp

9.3 Airborne Magnetometers

An FOM test performance of the CS-3 and fluxgate magnetometers was performed in order to monitor the ability of the system to remove the effects of aircraft motion on the magnetic measurement. The FOM maneuvers consisted of a series of calibration lines flown at high altitude (10,000ft+ above sea level). During this procedure, pitch, roll and yaw maneuvers were performed on the aircraft.

The following ranges were used:

Pitch: 10-15^{o}

Roll: 10-15^{o}

Yaw: 10-15^{o}

See Appendix B for the FOM results as flown on June 22nd, June 29th, 2010 and were used to compensate the magnetic data.

10.0 DATA COMPILATION

10.1 Flight Path Corrections

The navigational correction process yields a flight path expressed in WGS84, World and transformed to correspond to NAD 83 UTM ZONE 7N, North America. The flight line path for the airborne geophysical survey is shown in Figure 5.

10.2 Thorium Resolution Tests

A daily resolution test was carried out in order to monitor the resolution of the spectrometer. The results from the resolution tests were always found to be within the contract specifications.

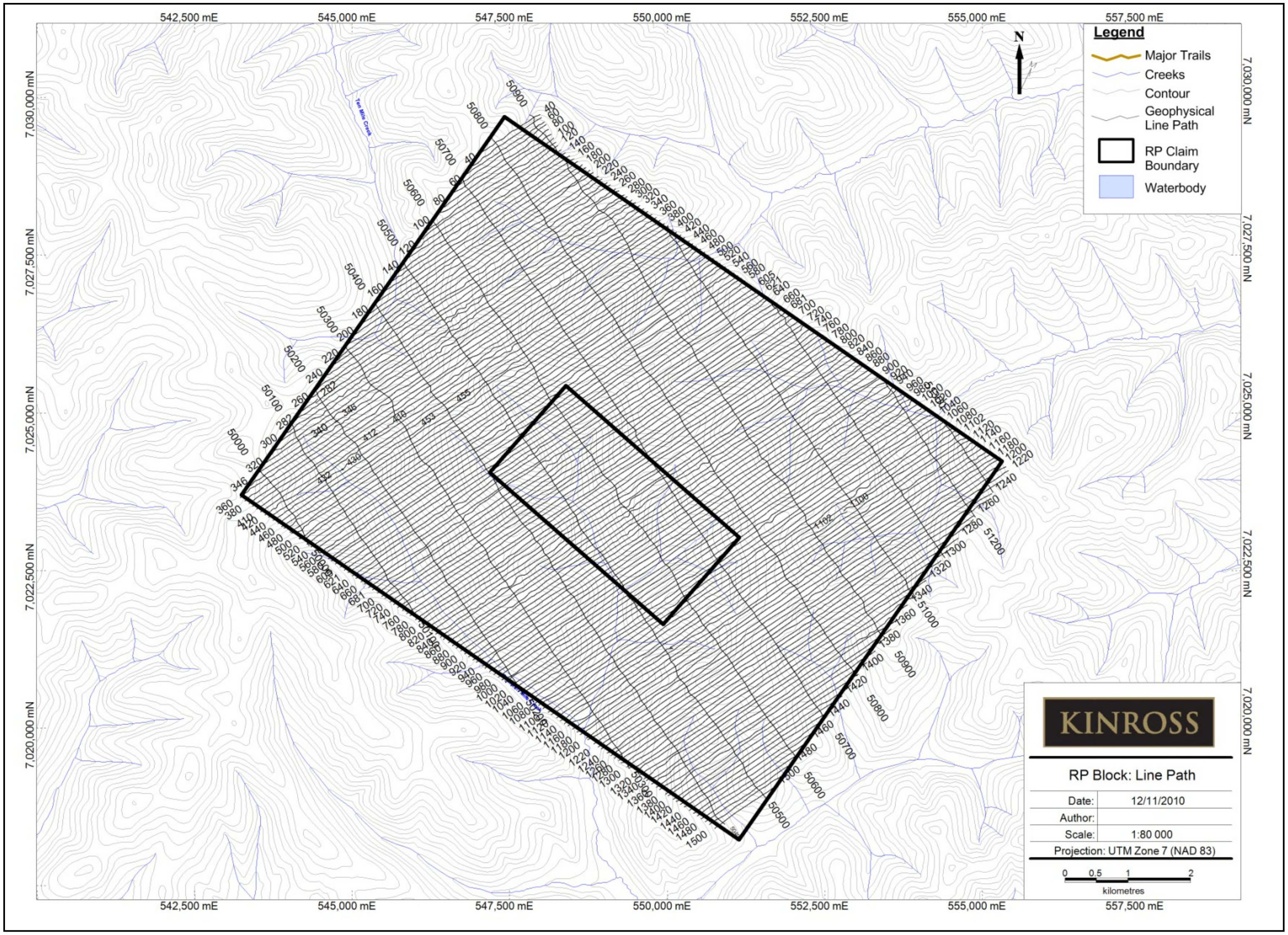

Figure 5: Flight Line Path for Airborne Geophysical survey over the RP Claim Block

10.2 Digital Terrain Model (DTM)

The DTM data was produced by first adjusting the GS sensor height to that of the radar altimeter height (lowering GPS height by 2.1 m). Next the radar altimeter channel (in metres) was subtracted from the GPS height data producing a raw DTM channel. Next the radar altimeter channel (in metres) was subtracted from the GPS height data producing a raw DTM channel. Because of inherent errors, the raw DTM channel required leveling. The following key microlevelling parameters were used (Table 9):

Block Name	Line Spacing (m)	Line Direction (deg.)	Grid Cell Size (m)	Decorrugation Cutoff (m)	Amplitude Limit (nT)	Amplitude Limit Mode	Naudy Filter Limit
RP	75	56	15	300	15	Clip	0

Table 9: DTM microlevelling parameters

The DTM contours produced from data collected during the airborne geophysical survey across the RP Claim Block are shown in Figure 6 and the final contoured and coloured DTM image shown in Figure 7.

Figure 6: Digital Terrain Model (DTM) Contours produced for the RP Claim Block

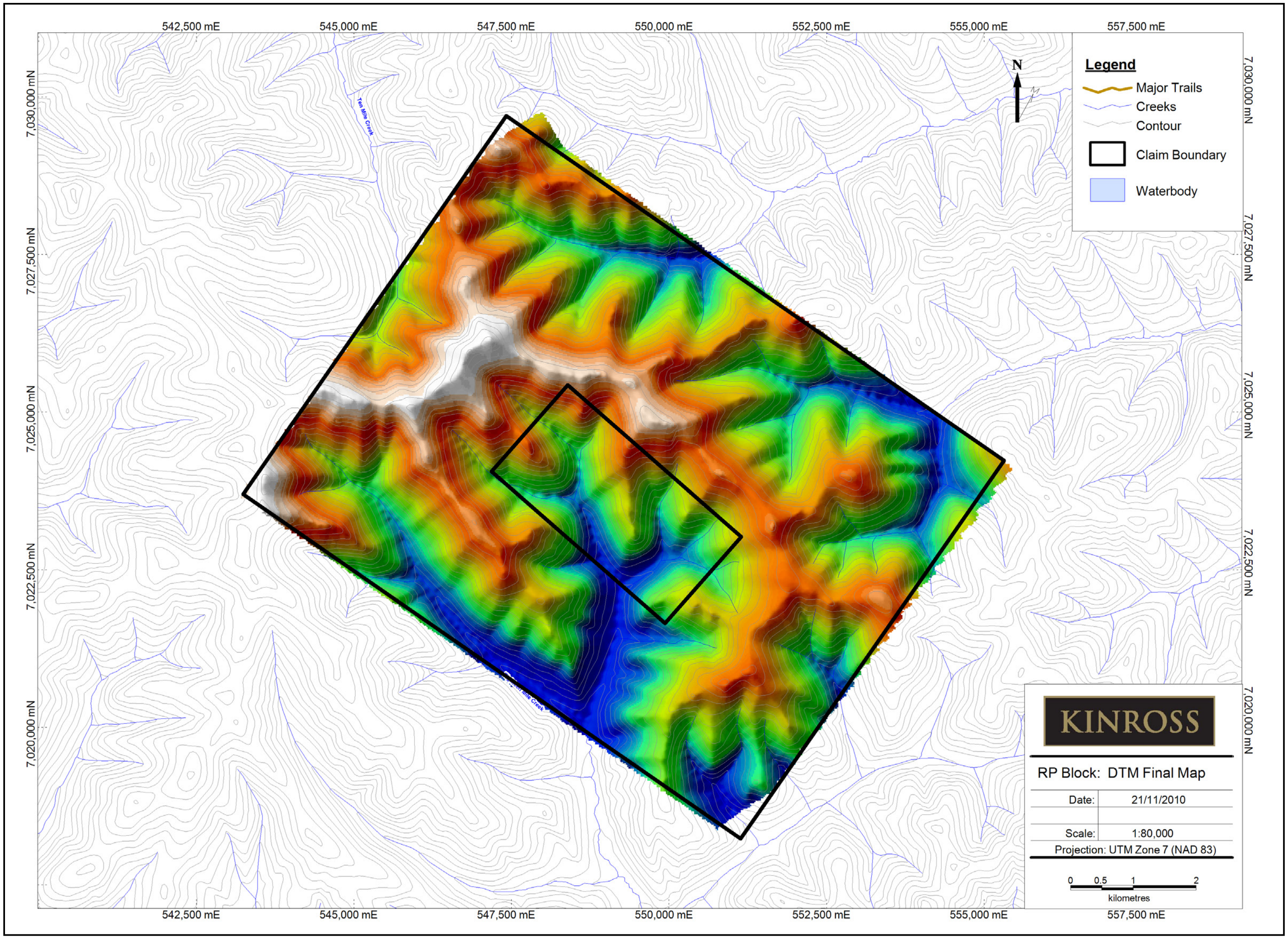

Figure 7: Map showing the final contoured Digital Terrain Model (DTM) map for the RP Block

10.3 Magnetic Corrections

The 50 Hz aeromagnetic data from Cesium 3 and Fluxgate magnetometers were filtered with a 51 cosine anti-aliasing algorithm and re-sampled at 10 Hz.

10.3.1 Diurnal Corrections

The compensated magnetic data were adjusted to account for diurnal variations. When the magnetic variation recorded at the base station recognized to be caused by manmade sources, such as equipment, vehicles passing by the sensor), they were removed and gaps interpolated. Diurnal variations recorded by the base station were filtered with a 101-point low pass filter. The filtered data was then subtracted directly from the aeromagnetic measurements to provide first order diurnal correction.

After base station removal, the total magnetic field values become very small. To bring the total magnetic measurements back to 'normal' values, project averages were added back to the magnetic data (Table 10).

Block Name	Average Readings (nT)
RP	57538.71

Table 10: Base Station Project Averages Per Block

10.3.2 Lag Corrections

There are two potential types of Lag offsets when collecting airborne data: time lag and distance lag. The distance lag is determined by dividing the distance from the GPS antenna to the sensor head by the averaged sample rate distance (Table 11).

Block Name	Distance from GPS Antenna to Sensor Head (m)	Average Sample Interval (m)	Lag Applied to Magnetic Data (records)
RP	9.2	2	-4

Table 11: Lag Corrections for RP Block

10.3.3 Heading Corrections

Optically pumped magnetic sensors have and inherent heading error, typically 1 to 2 nT peak-to-peak, as the sensor is rotated through 360 degrees.

Two heading test flights were flown at magnetically quiet area at 10,000 +ft above sea level altitude on June 24th and June 29th, 2010 with the following results (Table 12 and Table 13):

Line	Direction (deg.)	Mean on line (nT)	Mean in direction (nT)	Mean on heading (nT)	Error (nT)
	0				2.547
15	56	57157.66	57157.26	57155.40	-1.86
17	56	57156.85			
14	236	57153.20	57153.55		1.86
16	236	57153.89			
24	146	57160.55	57160.58	57155.36	-5.22
26	146	57160.61			
25	326	57150.24	57150.14		5.22
27	326	57150.04			

Table 12: Heading Test Flight Results: June 24th, 2010

Line	Direction (deg.)	Mean on line (nT)	Mean in direction (nT)	Mean on heading (nT)	Error (nT)
					-3.55
22	56	57235.40	57235.36	57232.95	-2.41
24	56	57235.32			
23	236	57228.86	57230.55		2.41
25	236	57232.23			
14	146	57227.91	57227.61	57231.85	4.24
16	146	57227.30			
13	326	57235.21	57236.09		-4.24
15	326	57236.97			

Table 13: Heading Test Flight Results: June 29th, 2010

10.3.4 IGRF Corrections

The total field strength of the International geomagnetic Reference Field (IGRF) was calculated for every data point, based on spot values of Latitude, Longitude and altitude. This IGRF was removed from the measured survey data on a point-by-point basis from the lag corrected channel. After IGRF correction the total magnetic field values become negative. The bring the total magnetic measurements back to ‘normal’ values an average of IGRF values based on the whole project were added back to the magnetic data (Table 14).

Block Name	Average Readings (nT)
RP	57278.31

Table 14: IGRF Averages for the RP Block

10.3.5 Leveling Corrections

After the data were corrected for IGRF, a survey control line intercepts matrix was created for determining differences in magnetic field at the intersection points. The same key parameters were used as shown in Table 9.

10.4 Vertical derivative

A 1-st Order vertical Derivative (VDV) data were calculated using 2D FFT2 algorithm based on final TMI grid. The resulting VDV grid was the filtered with a Hanning 3x3, with 2 passes, filter and sampled back to the database (Figure 8).

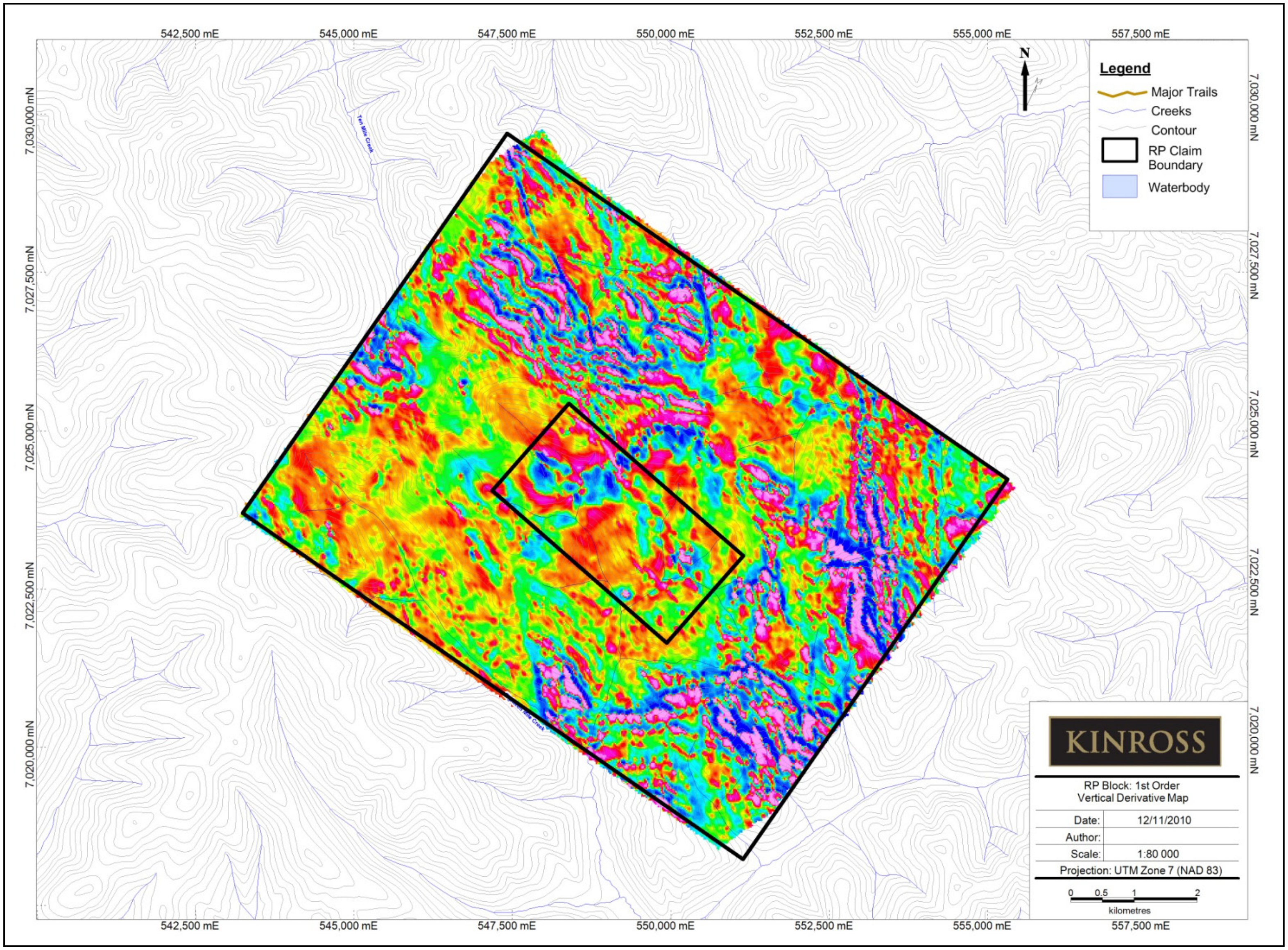

Figure 8: Map of the RP Block showing the final 1st-Order Vertical Derivative (VDV) Map

10.5 Radiometric Corrections

10.5.1 Live Time Corrections

The spectrometer uses the notion of 'live time' to express the relative period of time the instrument was able to register new pulses per sample interval.

The live time correction is applied to the total count, potassium, uranium, thorium and upward uranium channels.

The formula used to apply the correction is as follows:

$$C_{LT} = C_{raw} \times \left(\frac{1000}{LT} \right)$$

Where:

- C_{LT} is the live time corrected channel
- C_{raw} is the raw channel
- LT is the Live Time channel

10.5.2 Pre-Filtering

The cosmic channel data were processed with a 15-point low pass filter to remove spikes. When radon corrections were applied, live time, background and cosmic corrected uranium, thorium, and upward uranium were pre-filtered with 11, 11 and 21 point low pass filters respectively. The radar altimeter channel while recorded at 50Hz was filtered with 21-point COSINE filter and then sampled to 1Hz.

10.5.3 Aircraft and Cosmic Background

Aircraft background and cosmic stripping corrections were applied to the live corrected total count, potassium, uranium, thorium and upward uranium channels using the following formula:

$$C_{ac} = C_{LT} - (ac + bc \times cof)$$

Where:

- C_{ac} is the background and cosmic corrected channel
- C_{LT} is the live time corrected channel
- ac is the aircraft background for this channel
- bc is the cosmic stripping coefficient for this channel
- cof is the filtered cosmic channel

All negative counts after this correction step were replaced with zeroes.

10.5.4 Radon Correction

The relationships between the counts in the downward uranium window and on the four other windows (i.e., upward uranium, thorium, potassium and total count) due to atmospheric radon were determined using linear regression for the test site

The equations solved were:

$$u_r = a_u \times U_r + b_u$$

$$K_r = a_K \times U_r + b_K$$

$$T_r = a_T \times U_r + b_T$$

$$I_r = a_I \times U_r + b_I$$

Where:

- u_r is the radon component in the upward uranium window
- K_r, U_r, T_r and I_r are the radon components in the various windows of the downward detectors
- The various "a" and "b" coefficients are the required calibration constants

The radon component in the downward uranium window was then determined using the following formula:

$$U_r = \frac{(u_f - a_1 \times U_f - a_2 \times Th_f + a_2 \times b_r - b_u)}{(a_u - a_1 - a_2 \times a_r)}$$

Where:

- U_r is the radon component in the downward uranium window
- u_f is the filtered upward uranium
- U_f is the filtered uranium
- Th_f is the filtered thorium
- a_1, a_2 are proportionality factors
- b_u and b_r are background constants

10.5.5 Compton Stripping

Following the background and cosmic corrections (above) the potassium, uranium and thorium were corrected for spectral overlap.

The stripping corrections are then carried out using the following formulas:

$$ar = \frac{1}{1-a\alpha h}$$

$$Th_c = (Th_{bc} - aU_{rc}) \times ar$$

$$U_c = (U_{rc} - Th_{bc}\alpha h) \times ar$$

$$K_c = K_{bc} - \beta h Th_c - \chi h U_c$$

Where:

- U_c, Th_c, and K_c are corrected Uranium, Thorium and Potassium
- ah, βh, and χh are the height corrected Compton stripping coefficients
- U_{rc}, Th_{bc} and K_{bc} are background and comic corrected Uranium, Thorium and Potassium
- ar is the backscatter correction
- a is the reverse stripping ratio U into Th

All negative counts after this correction were replaced with zeroes.

10.5.6 Attenuation Corrections

The Total Count, Potassium, Uranium and Thorium data were then corrected to a nominal survey altitude of 30 m using the following equation:

$$C_a = C \times e^{-\mu(h_0 - h_e)}$$

Where:

- C_a is the output altitude corrected channel
- C is the input channel
- μ is the attenuation correction for that channel
- h_e is the STP height
- h_0 is the nominal survey altitude

10.5.6.1 Leveling of Attenuation Corrected data

The altitude attenuation corrected data for all the Traverse lines were further microleveled with the following key parameters:

Block Name	Line Spacing (m)	Line Direction (deg.)	Grid Cell Size (m)	Decorrugation Cutoff (m)	Amplitude Limit (nT)	Amplitude Limit mode	Naudy Filter Limit
RP	75	56	15	300	30	Clip	100

Table 15: Uranium microlevelling parameters

Block Name	Line Spacing (m)	Line Direction (deg.)	Grid Cell Size (m)	Decorrugation Cutoff (m)	Amplitude Limit (nT)	Amplitude Limit mode	Naudy Filter Limit
RP	75	56	15	300	15	Clip	0

Table 16: Thorium microlevelling parameters

Block Name	Line Spacing (m)	Line Direction (deg.)	Grid Cell Size (m)	Decorrugation Cutoff (m)	Amplitude Limit (nT)	Amplitude Limit mode	Naudy Filter Limit
RP	75	56	15	300	15	Clip	100

Table 17: Potassium microlevelling parameters

Block Name	Line Spacing (m)	Line Direction (deg.)	Grid Cell Size (m)	Decorrugation Cutoff (m)	Amplitude Limit (nT)	Amplitude Limit mode	Naudy Filter Limit
RP	75	56	15	300	200	Clip	100

Table 18: Total Count microlevelling parameters

10.5.6.2 Ternary Map

The radioelement ternary map was produced by creating individual grids for the three radioelements (potassium, thorium and uranium), then assigning a colour to each. Cyan represents thorium, yellow uranium, and magenta potassium. The relative concentrations of the radioelements are represented by the blending of the three colours (Figure 16).

11.0 RESULTS AND INTERPRETATION

The results and maps included with this report display the magnetic and radiometric properties of the geophysical survey area. The combination of geophysics and regional geological information allows some general correlations to be made.

11.1 Magnetics

The Total Magnetic Intensity (TMI) final map was one of the main products from the high resolution airborne survey flown across the RP Block (Figure 10). Anomalies identified from the colour-shaded TMI map are presented herein: The most striking features from the compilation of the magnetic data for the RP Claim Block are the dominant northwest-southeast trending lineaments and magnetic highs in the northwestern part of the Claim Block (Figure 10). Amphibolite gneiss units typically crop out on ridge tops, the northwest-southeast trending magnetic high observed in the northwest corner of the RP Claim block may be attributed to such outcrops (Figure 10). This amphibolite gneiss unit is interpreted to dip to the south/southwest, based on the broad and gradual decrease in the TMI to the south. This correlates well with the structural measurements from geological mapping by Ryan and Gordey in 2004. The amphibolite gneiss unit to the south does not appear to have the same structural orientation. While the conglomerate situated proximal to the amphibolite gneiss appears to be dipping in a more southeastern orientation. A small ultramafic body may be giving the magnetic highs centred at 552300Em and 7024700N (Figure 10).

Using the 1st-Order Vertical Derivative (Figure 8) the survey is potentially less-sensitive to noise in the data. When compared to the TMI image for the RP Block (Figure 10), the 1st-Order VDV image (Figure 8) provides a close association between distinctively magnetic high areas; particularly in the northwest/southeast trending high areas in the northern part of the claim block and the southeast corner. Such a strong correlation is not observed for the relatively high magnetic anomaly along the southern margin of the RP Claim Block (Figure 10).

Strong, diffuse magnetic highs, such as those observed in the southern corner of the claim block are likely a result of host bedrock geology. For the purposes of interpretation when the TMI image (Figure 10) is overlain over the regional geology map for the Stewart River area (Ryan and Gordey, 2004) several correlations stand out. Firstly intense magnetic responses correlate with areas of the claim block mapped as amphibolite gneiss by Ryna and Gordey (2004). Such intense magnetic responses can be invoked by ultramafic rocks, such as serpentinite bodies and amphibolite gneiss units. Regional geology studies (Ryan and Gordey, 2002; Paulsen et al., 2010) have mapped ultramafic bodies.

The geology of the southeast part of the claim block appears to be structurally complex with several interpreted lineaments cutting through areas that invoke magnetically high responses (Figure 10). These are likely attributed to regional -scale faults that disrupt the local geology or to contrasting lithological packages. A strong, linear magnetic low in the northeast corner of the RP Claims could be interpreted as a regional-scale thrust fault, similar to those mapped at the White Claims to the southeast. However, regional mapping by Ryan and Gordey (2004) did not record any large-scale faults on the RP property (Figure 11).

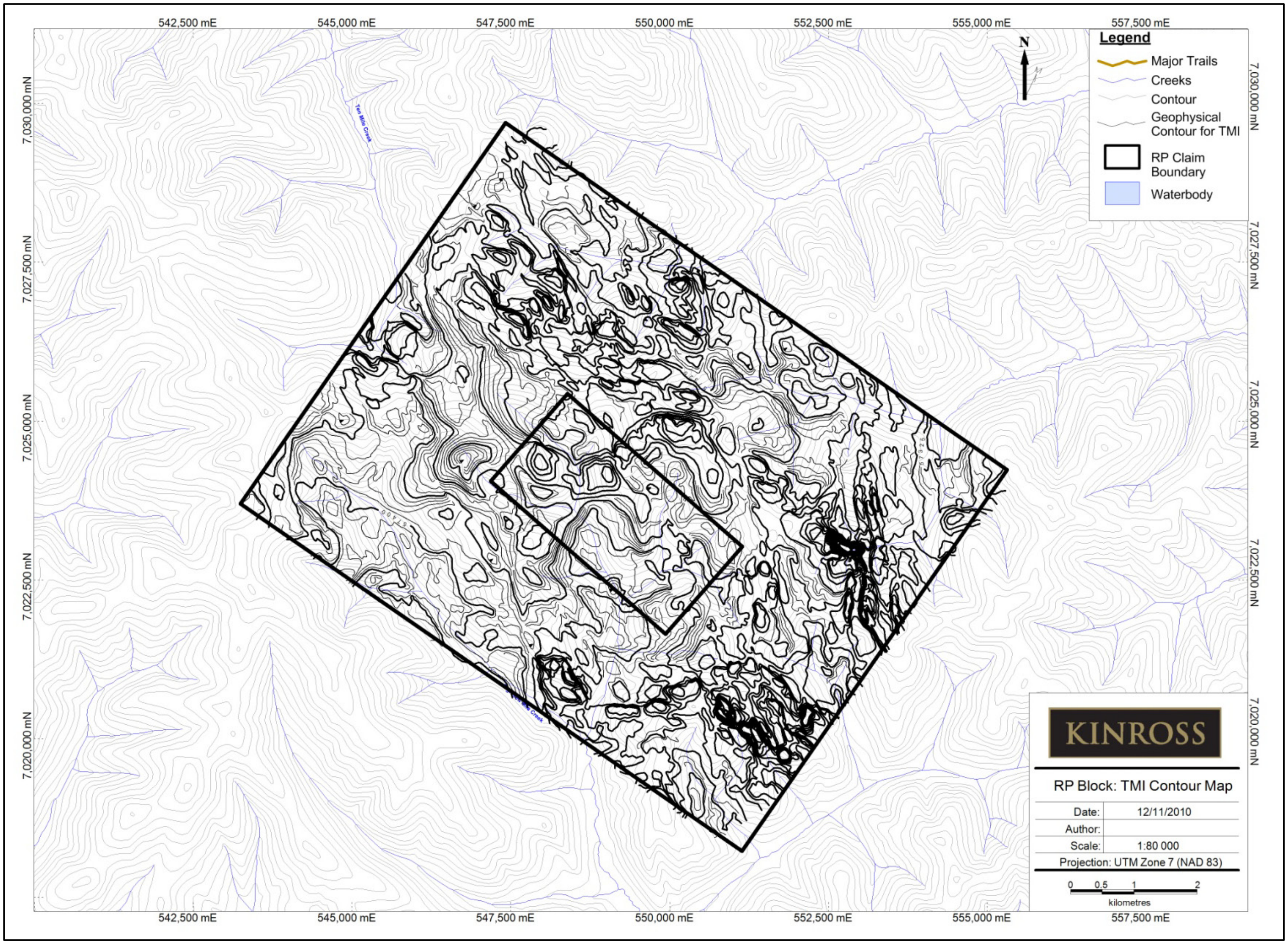

Figure 9: Total Magnetic Intensity (TMI) contour map for the RP Block

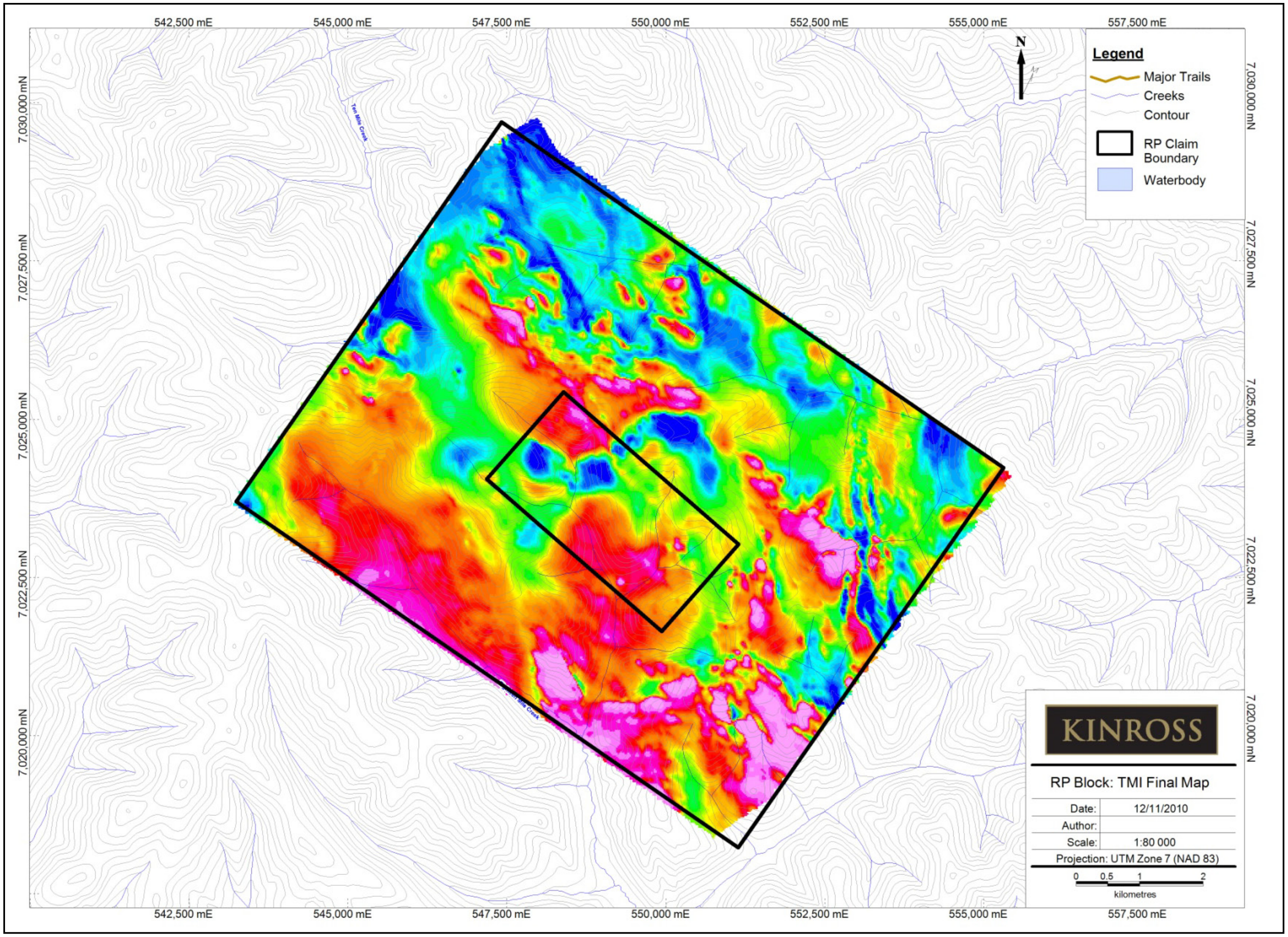

Figure 10: Final Total Magnetic Intensity (TMI) image for the RP Block. Traverse lines: 75m, 56/236 deg. From true North; Control Lines: 750 m, 146/326 deg. from true North. Average Sample Interval: 2.0 m/sample (10Hz), Average Sensor Height From Ground: 35.7 m.

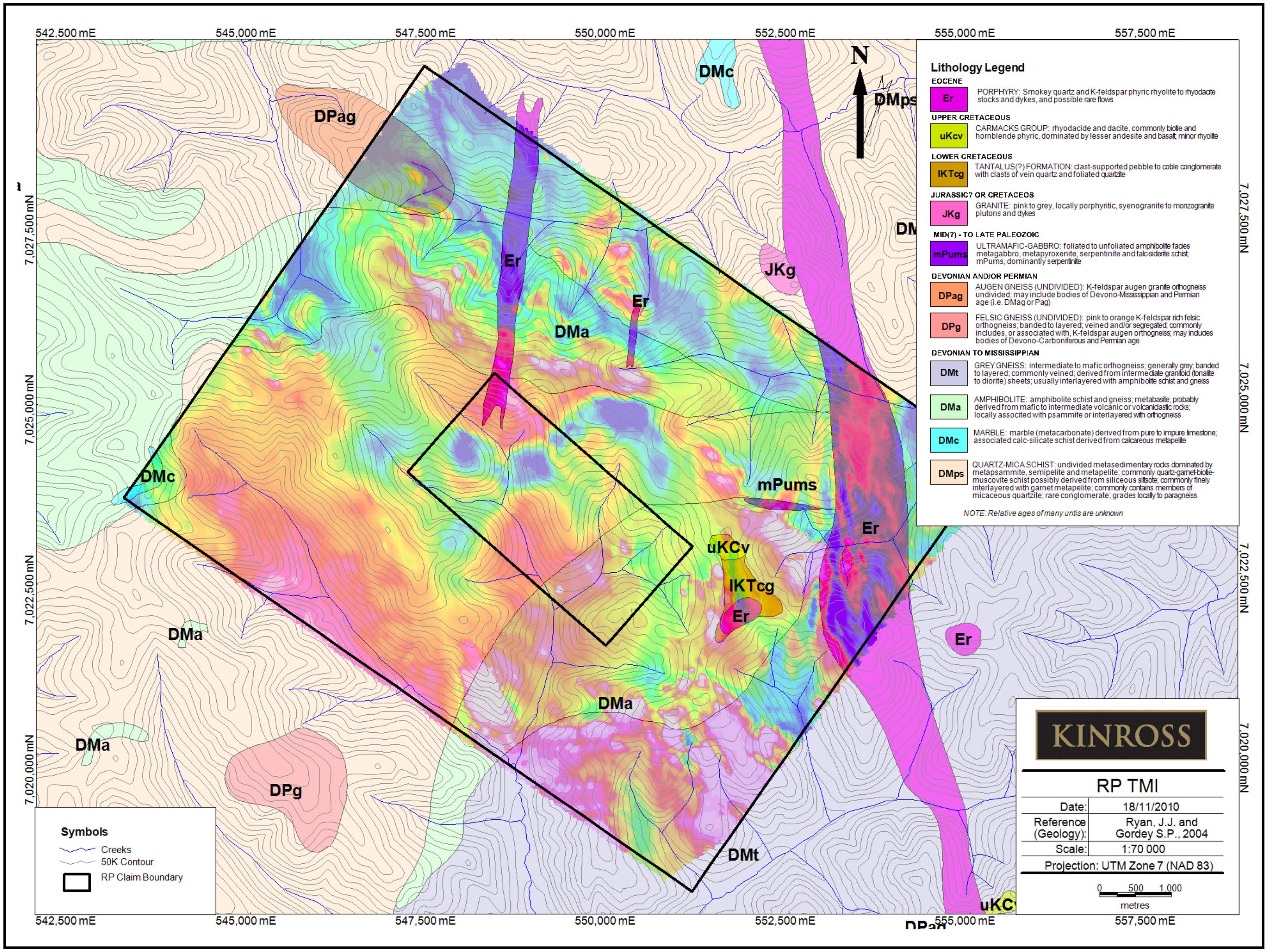

Figure 11: Final Total Magnetic Intensity (TMI) map for the RP Block, underlain with regional geology map (modified from Ryan and Gordey, 2004).

11.2 Radiometrics

High-sensitivity, quantitative gamma-ray spectrometry has been applied to the RP Block to aid mineral exploration on the property. The method depends upon the fact that absolute and relative concentrations of radioelements K, U and Th vary measurably and significantly with lithology.

The radiometric survey provided good resolution the RP Claim Block (Figure 12). In particular, the Potassium (K) map shows well-defined potassium highs. These distinct high areas are located in the eastern part of the RP Block; this corresponds well with mapped Eocene quartz porphyry (Figure 13). Central parts give lower, yet still anomalous potassium responses which are all mapped as muscovite schist by the GSC (Ryan and Gordey, 2004)(Figure 13). The potassium highs (anomalies) identified from the radiometric survey provided a good tool for potentially imaging felsic bodies across the claim block. These small bodies are primarily located on the eastern side of the property and measure approximately 500 m in diameter. While the lows also provide useful information and tend to show more mafic rich areas often corresponding to the amphibolite unit found with the RP claim block.

The Radiometric Potassium (K) map also images the relatively strong response of the potassium-rich interpreted muscovite schist units (central portion of the claim block) (Figure 12). In addition the block image of Thorium (Th) across the RP Claim Block correlates well with the aforementioned Potassium map (Figure 14). The Uranium(U) map produced for the RP Claims also displays a strong radiometric response at the western margin of the claim block (as seen in K and Th also)(Figure 15).

The Ternary Image map (Figure 16) for the RP Block emphasizes subtle distinctions in the relative concentrations of the radioactive elements, thereby ‘fingerprinting’ formations (Grasty et al., 1984). The ternary map shows a single colour image representing the relative concentrations of K (magenta), eU (cyan) and eTh (yellow) (Figure 16).

There are no coincident potassium anomalies and magnetic highs interpreted from the K map (Figure 12) and TMI map (Figure 10).

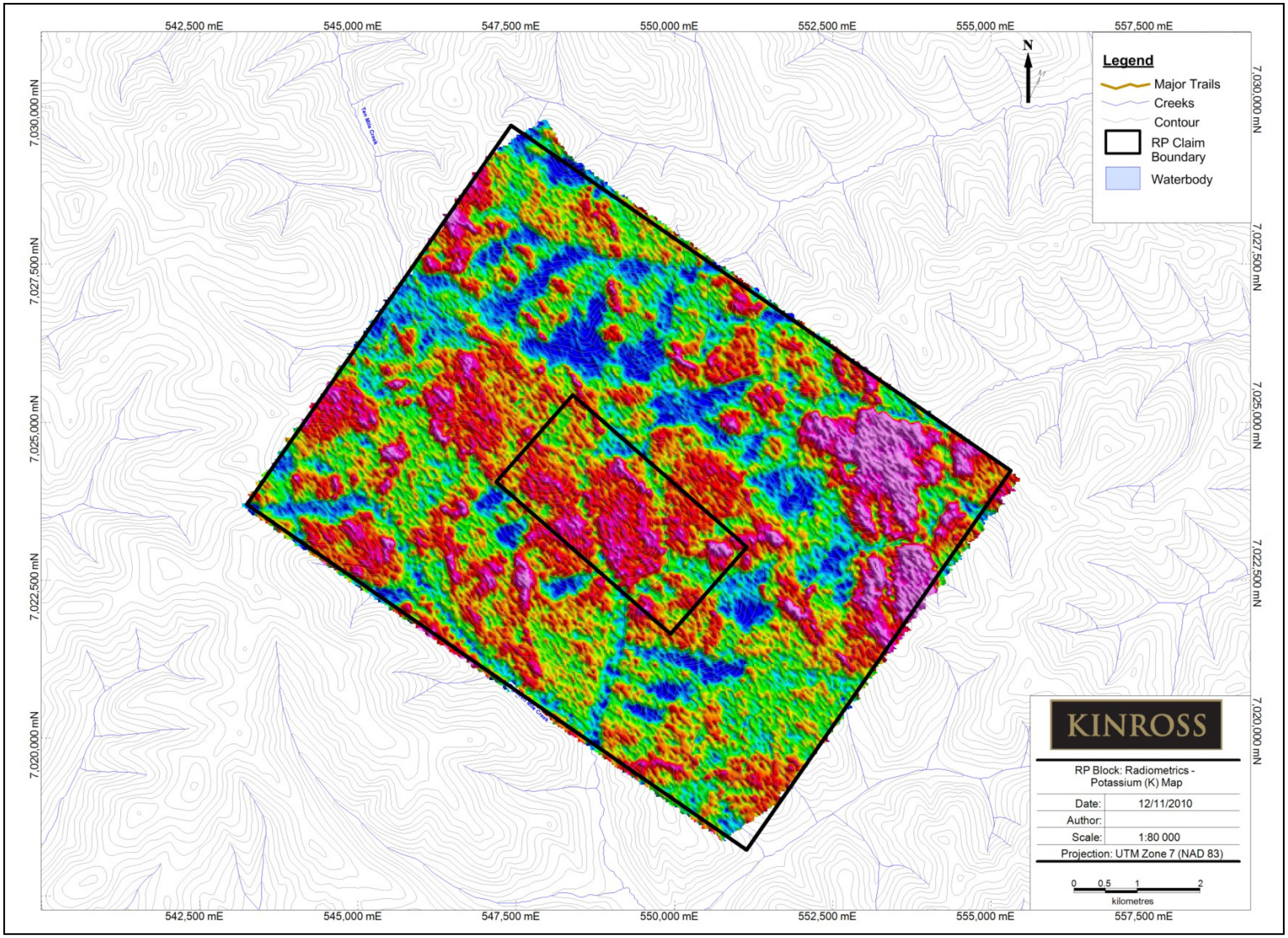

Figure 12: Final Potassium (K) map for the RP Block. Traverse lines: 75 m, 56/236 deg. From true North; Control lines: 750 m, 146/326 deg. From true North. Average Sample Interval: 20.0 m/sample (1Hz). Average Sensor Height From Ground: 36.0 m.

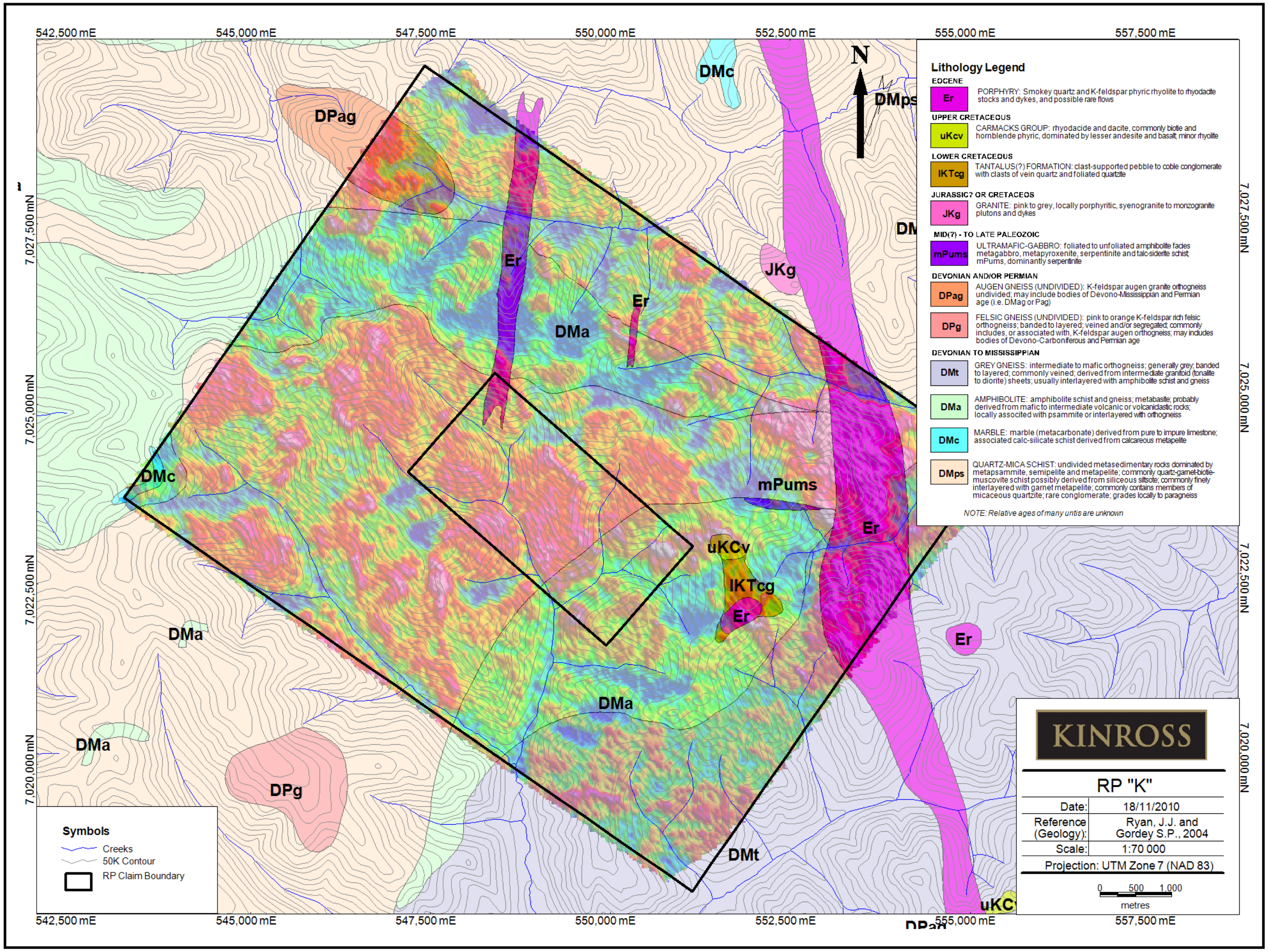

Figure 13: Final Potassium (K) map for the RP block, overlain by regional geology (modified from Ryan and Gordey, 2004).

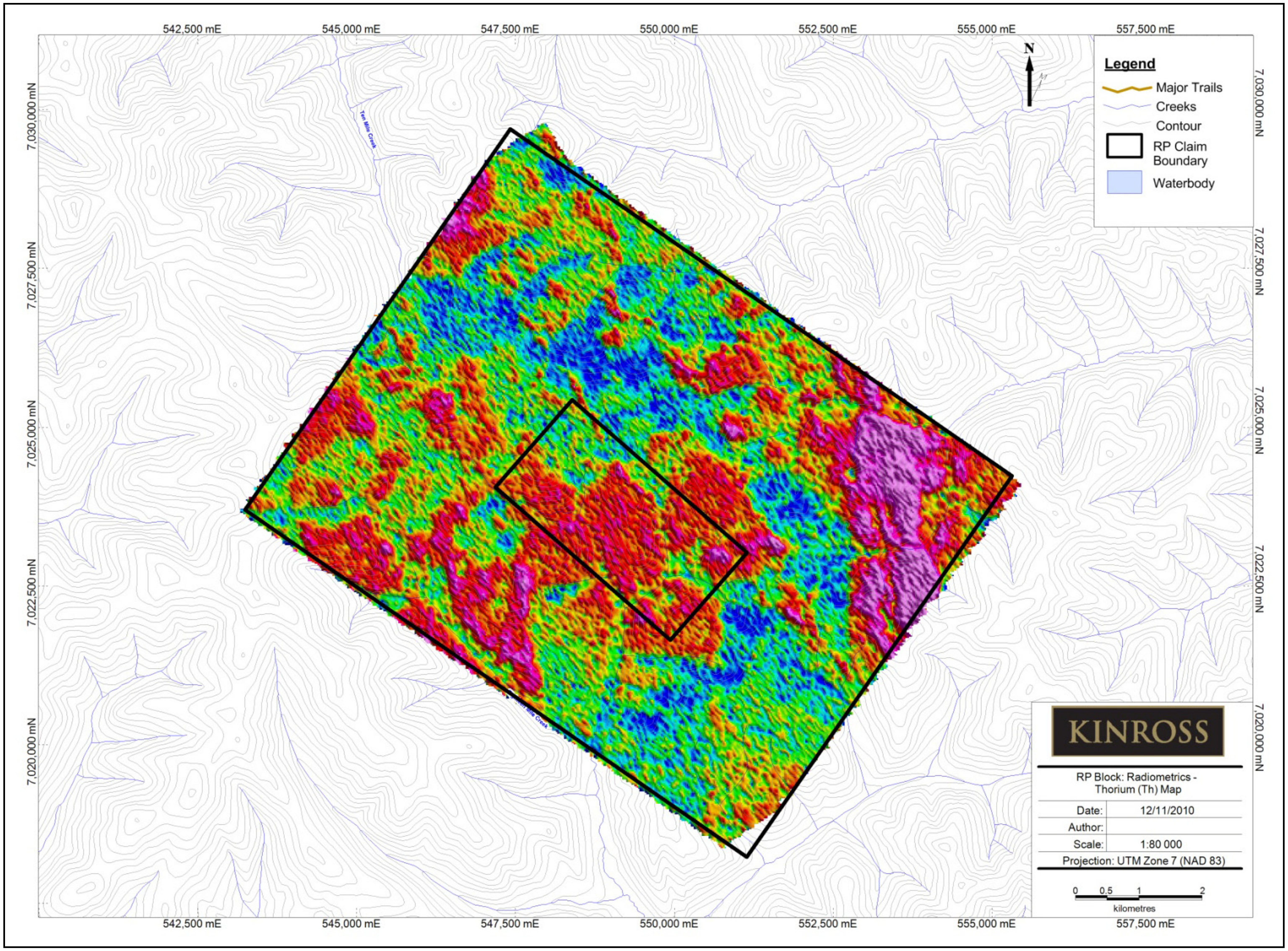

Figure 14: Final Thorium (Th) map for the RP Block. Traverse lines: 75m, 56/236 deg. From True North; Control Lines: 750 m, 146/326 deg. From True North. Average Sample Interval: 20.0 m/sample (1Hz). Average Sensor Height From Ground: 36 m.

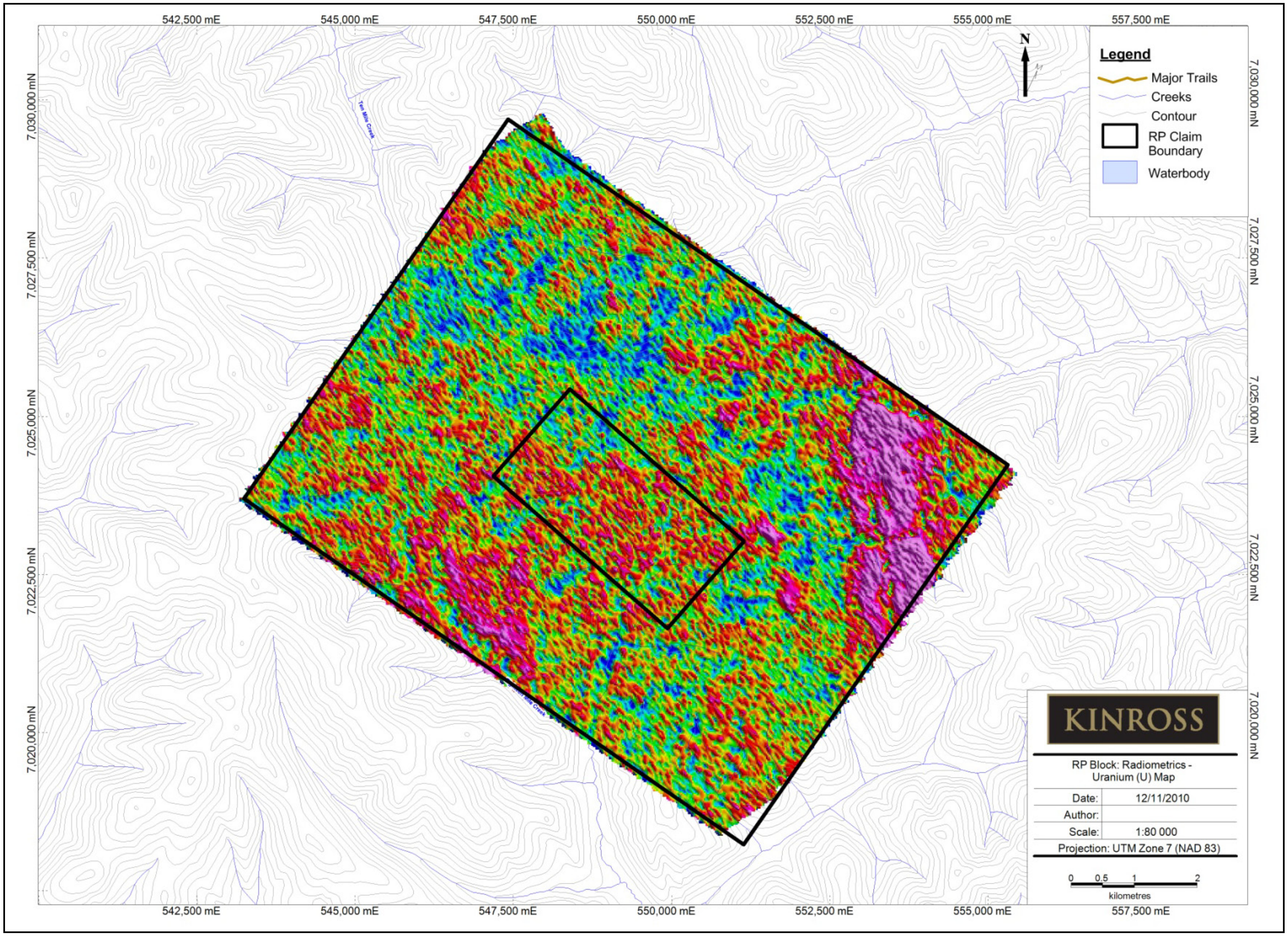

Figure 15: Final Uranium (U) map for the RP Block. Traverse lines: 75m, 56/236 deg. From True North; Control Lines: 750 m, 146/326 deg. From True North. Average Sample Interval: 20.0 m/sample (1Hz). Average Sensor Height From Ground: 36 m.

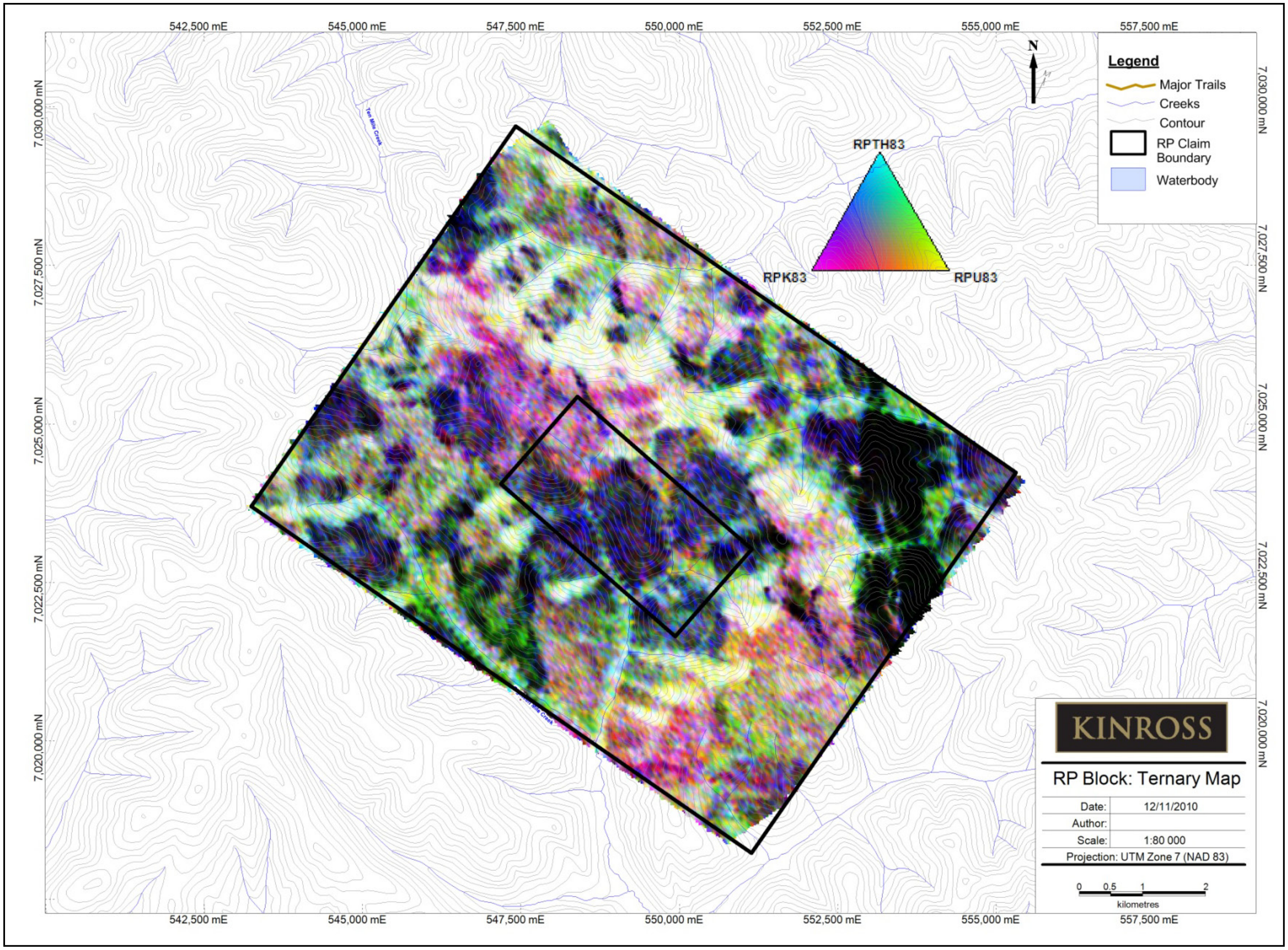

Figure 16: Final Ternary (K-eU-eTh) image map for the RP Block. Traverse lines: 75m, 56/236 deg. From True North; Control Lines: 750 m, 146/326 deg. From True North. Average Sample Interval: 20.0 m/sample (1Hz). Average Sensor Height From Ground: 36 m.

12.0 DISCUSSION & CONCLUSIONS

The RP Claim Block is a helicopter-accessible property in the White Gold District of the Yukon Territory. It comprises 336 full-size quartz claims; RP 1 through 336. The claim block represents a relatively under-explored part of the White Gold District. Owing to vegetation cover, and lack of surface outcrop the high-sensitivity airborne geophysical survey represents a first-step to mineral exploration and the development of a geological context for the property.

The high-sensitivity airborne geophysical survey conducted across the RP Claim Block during summer 2010 provides the only geophysical data for the RP property. The 2010 survey provided detailed images of potassium, uranium and thorium enrichment or depletion across the survey block. These images will be used as exploration tools to further mineral exploration at the property-scale.

Further data processing and refined presentation methods may enhance interpretations made herein. The magnetic and radiometric data collected must be applied to a constrained geological model in order to fully process the results. But as a first pass, the final TMI, DTM, VDV and K, U and Th maps are a good basis for further exploration, especially when used in conjunction with regional historical mapping (Figure 11 and Figure 13).

The radiometric K-U-Th image maps and the ternary map for the RP Claim Block provided good image resolution for interpretation of property-scale host rocks and particularly intrusive rock types, (K-high areas) as shown by the correlation of Eocene porphyry intrusive rocks (previously mapped by Ryan and Gordey (2004) with areas of high potassium (Figure 13).

The gradient from higher values in the south to lower in the north indicates a lithologic change in bedrock composition. The magnetic high signatures may represent lithologic contacts or intrusive relationships and require more-detailed follow-up ground work (Figure 11).

Considering the proximity of the RP Claim Block to the White Gold district and the Golden Saddle Deposit plus other significant gold showings and occurrences, additional prospecting and geochemical soil and rock sampling is warranted for the future.

Statement of Expenditures on the RP (1-336) Claims

Details

Contract Services

Field Personnel: New-Sense Geophysical Ltd. Equipment/Survey & Report	$35,864
Total Expenditure 2010 Airborne Survey/RP Block	**$35,864**

References

Dusel-Bacon, C. (2006): Paleozoic tectonic and metallogenic evolution of the pericratonic rocks of east-central Alaska and adjacent Yukon. In Paleozoic evolution and Metallogeny of Pericratonic Terranes at the Ancient Pacific Margin of North America, by M.Colpron and J.Nelson, 25-74. Geological Association of Canada Special Paper 45.

Grasty, R.L., Carson, J.M., Charbonneau, B.W., and Holman, P.B. (1984): Natural background radiation in Canada. Geological Survey of Canada Bulletin 360, 39pp.

Mackenzie, D. and Craw, D. (2009): Structural controls on hydrothermal gold mineralization in the White River area, Yukon. Yukon Exploration and Geology: 253-263.

Mortensen, J.K. (1992): Pre-mid Mesozoic tectonic evolution of the Yukon-Tanana terrane, Yukon and Alaska. *Tectonics 11*: 836-853.

Paulsen, H-K., Gibson, J., Fleming, A., and King, N. (2010): Technical Report on the White Gold Property, Dawson Range, Yukon. Unpublished Underworld Resources Inc, in 2009 Annual Report.

Ryan, J.J., and Gordey, S.P. (2002): Bedrock geology of Yukon-Tanana terrane in southern Stewart River map area, Yukon Territory. *Geological Survey of Canada Current Research 2002-A1.*

Ryan, J.J., and Gordey, S. (2004): Geology, Stewart River Area (Parts of 115N/1,2,7,8, and 115-O/2-12, Yukon Territory, Geological Survey of Canada, Map 1772A, scale 1:100 000.

Yakovenko, A. (2010): Logistics Report for the high Resolution Helicopter Magnetic and Gamma-ray Spectrometric Airborne Geophysical Survey. New-Sense Geophysics Ltd. Report published for Kinross Gold Corp.

APPENDIX A: Background and Cosmic Test Charts

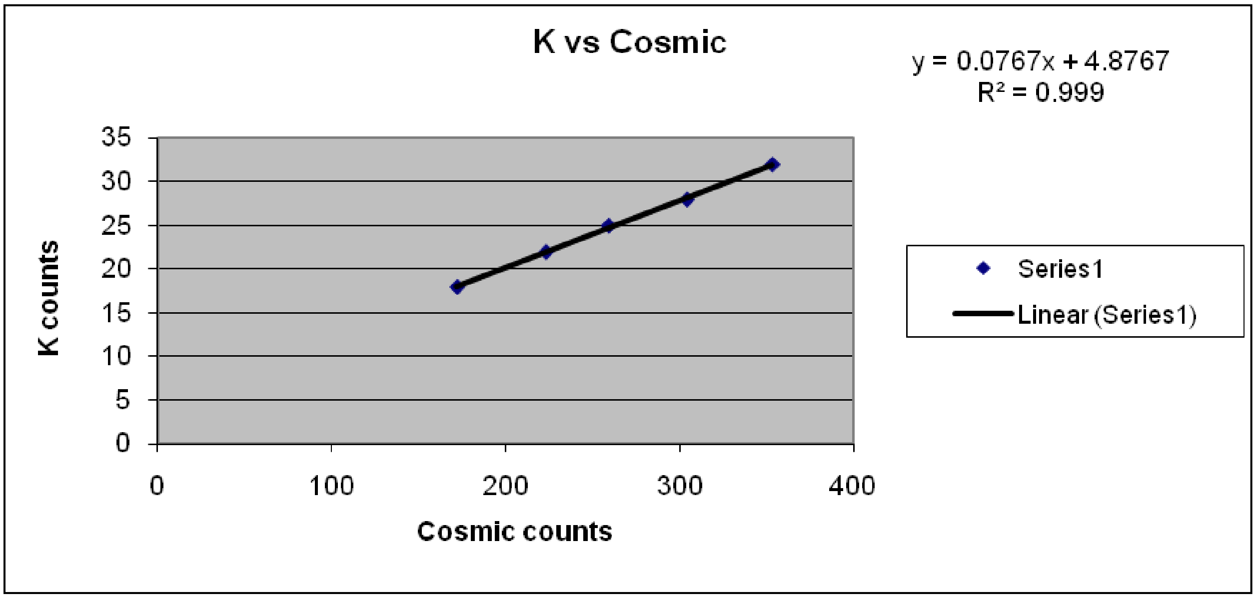

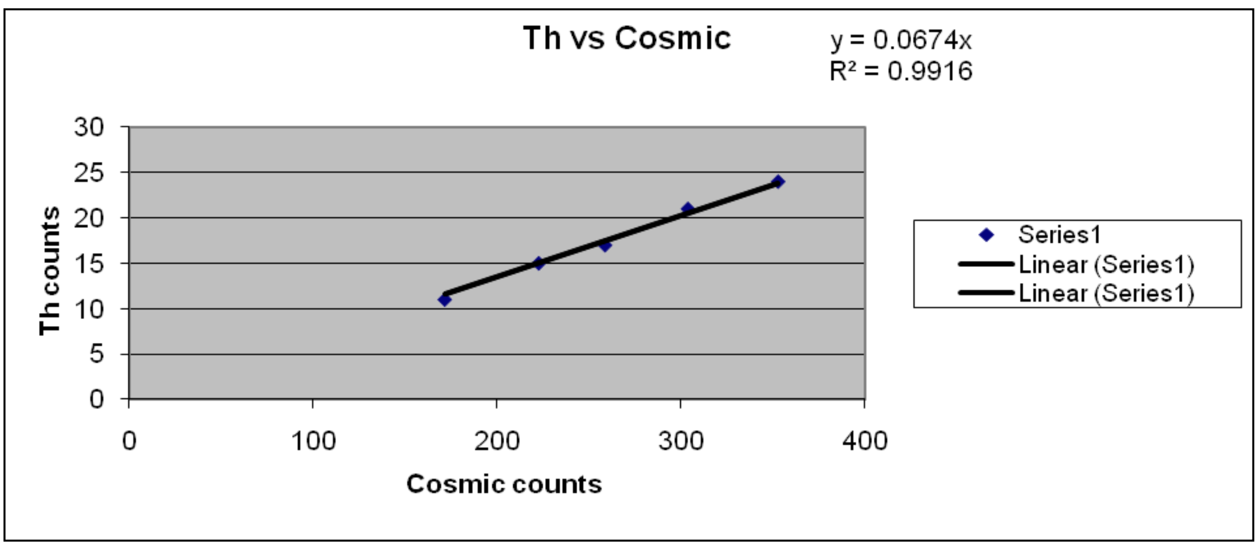

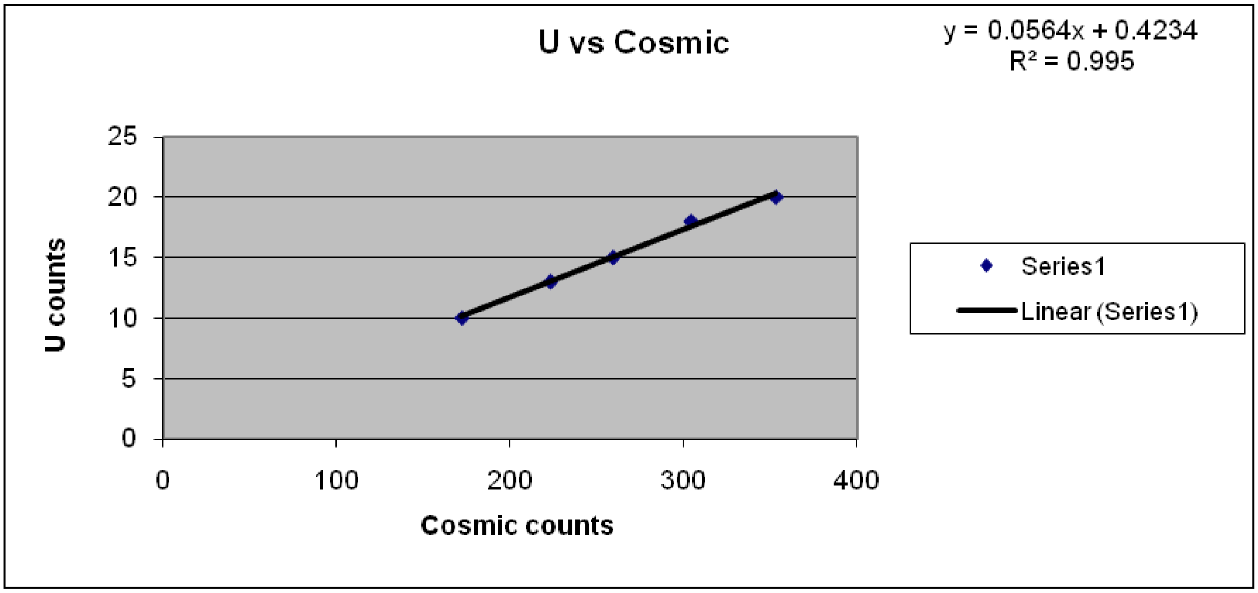
U vs Cosmic
y = 0.0564x + 0.4234
R² = 0.995
U counts
25
20
15
10
5
0
0
100
200
300
400
Cosmic counts
Series1
Linear (Series1)

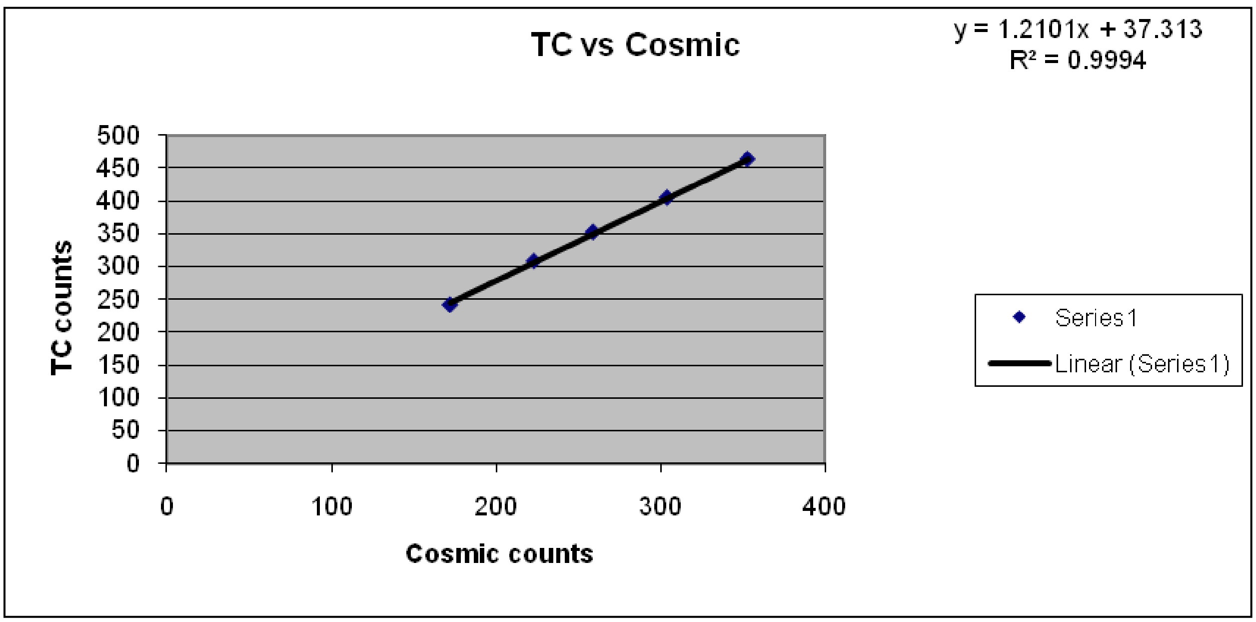
TC vs Cosmic
y = 1.2101x + 37.313
R² = 0.9994
TC counts
500
450
400
350
300
250
200
150
100
50
0
0
100
200
300
400
Cosmic counts
Series1
Linear (Series1)

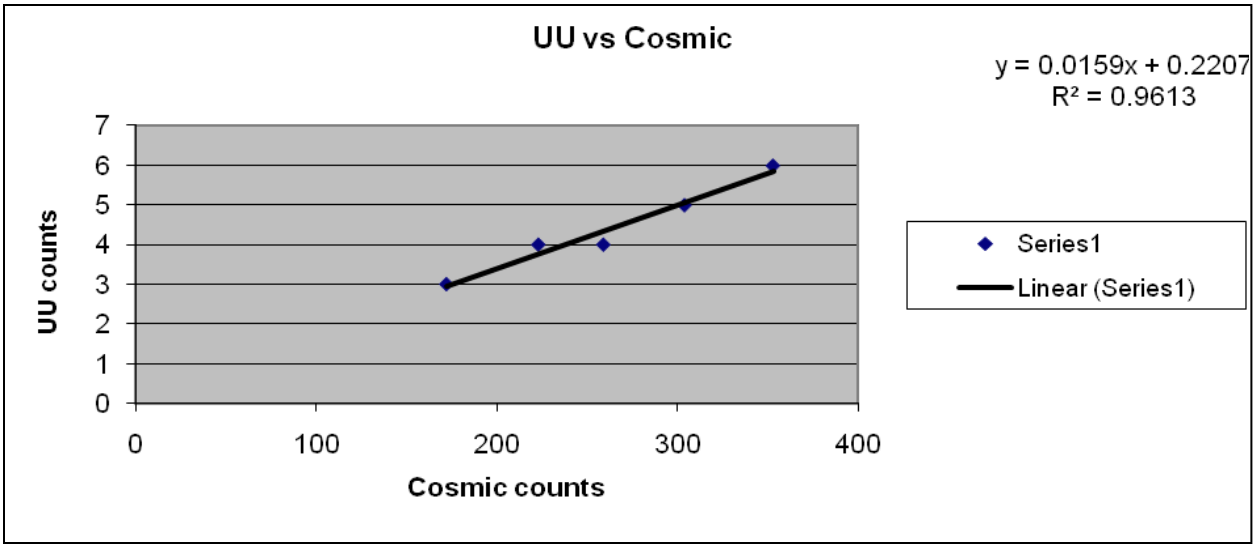
UU vs Cosmic
y = 0.0159x + 0.2207
R² = 0.9613
UU counts
Cosmic counts
0
1
2
3
4
5
6
7
0
100
200
300
400
Series1
Linear (Series1)

Height Attenuation Test Charts

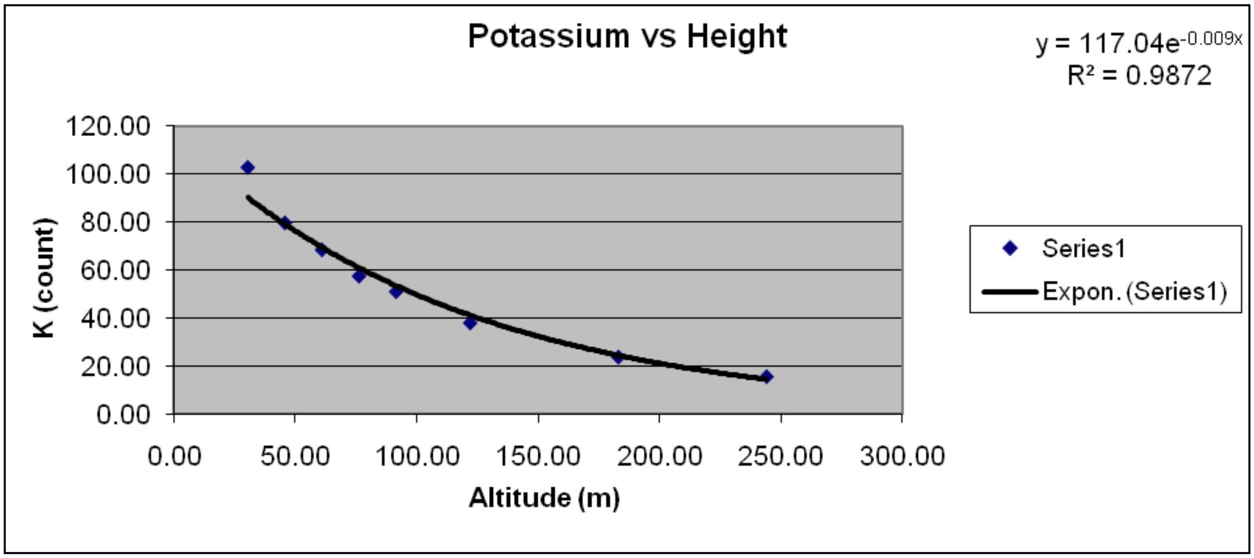

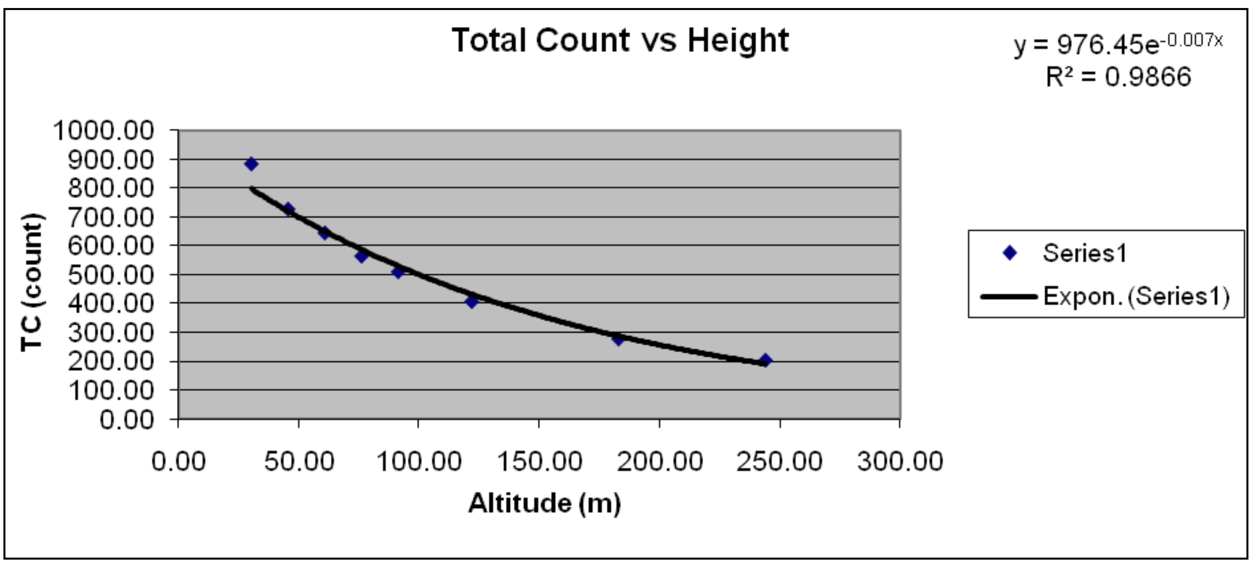

APPENDIX B: Fom Results

Kinross Gold, Yukon, FOM, June 22nd, 2010					
Line	**Direction**	**Pitch**	**Roll**	**Yaw**	**Total**
1000	**236**	0.100	0.100	0.100	0.300
2000	**56**	0.150	0.100	0.100	0.350
3000	**146**	0.100	0.085	0.130	0.315
4000	**326**	0.110	0.125	0.125	0.360
	Total	0.460	0.410	0.455	1.325

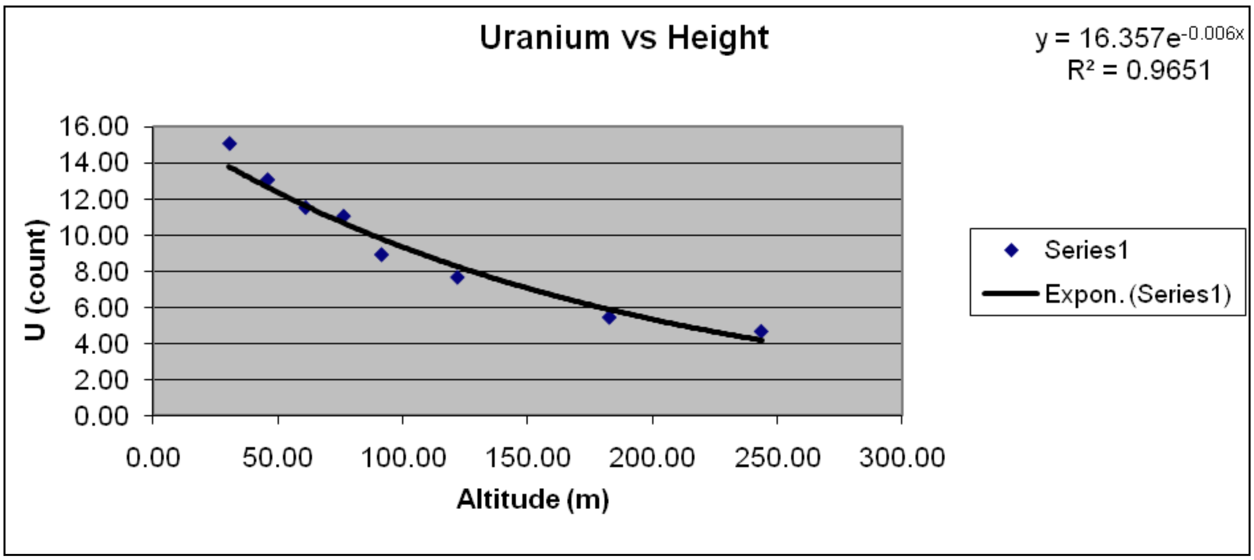

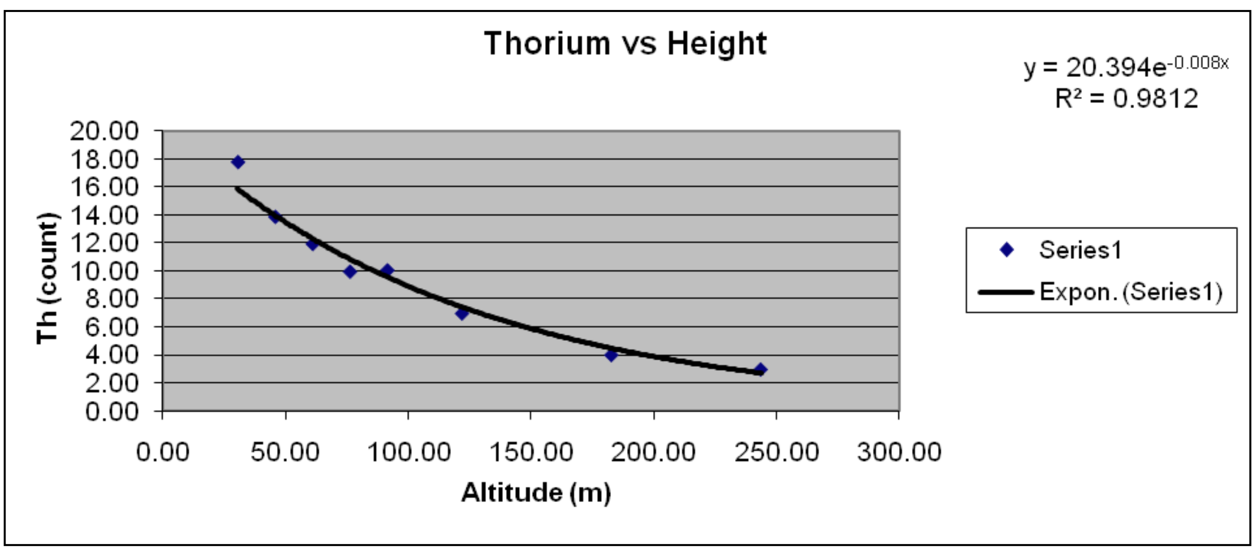

Statement of Qualifications

I, Lucy Hollis, Vancouver, B.C. do hereby certify that:

- I am a Geologist in the employment of Kinross Gold Corporation, within the Vancouver office at 1380 West Georgia, Vancouver, B.C.
- I am a graduate of the University of Birmingham, UK, with an M.Sci in Geology (with an International Year) and University of British Columbia, Vancouver, Canada with a M.Sc in Geological Science.
- I have been involved in exploration geology in Canada for the past four years and have been employed by Kinross Gold Corp since April 2009.
- This report is compiled from the given references and the authors personal experience.

L.Hollis, M.Sci, M.S

Legend
Major Trails
Creeks
Contour
Claim Boundary
Waterbody
RP Claims
EMC Claims
YC97170 Grant Number
RP 170 Claim Label
N
Ten Mile Creek
Eighteen Mile Creek
Eighteen Mile Creek
White River
White River
117,500 mE
120,000 mE
122,500 mE
125,000 mE
127,500 mE
130,000 mE
1,012,500 mN
1,010,000 mN
1,007,500 mN
1,005,000 mN
1,002,500 mN
1,000,000 mN
997,500 mN
995,000 mN
992,500 mN
KINROSS
RP Claims
Date: 10/11/2010
Scale: 1:30 000
Projection: UTM Zone 7 (NAD 83)
0 0.5 1 2
kilometres